REVIEW

Check for updates

Design of hydrogel-based wearable EEG electrodes for medical applications

Ju-Chun Hsieh, [iD] †[a] Yang Li, [iD] †[b] Huiqian Wang,[c] Matt Perz,[a] Qiong Tang,[d] Kai Wing Kevin Tang,[a] Ilya Pyatnitskiy, [iD] [a] Raymond Reyes,[a] Hong Ding[a] and Huiliang Wang [iD] *[a]

The electroencephalogram (EEG) is considered to be a promising method for studying brain disorders. Because of its non-invasive nature, subjects take a lower risk compared to some other invasive methods, while the systems record the brain signal. With the technological advancement of neural and material engineering, we are in the process of achieving continuous monitoring of neural activity through wearable EEG. In this article, we first give a brief introduction to EEG bands, circuits, wired/wireless EEG systems, and analysis algorithms. Then, we review the most recent advances in the interfaces used for EEG recordings, focusing on hydrogel-based EEG electrodes. Specifically, the advances for important figures of merit for EEG electrodes are reviewed. Finally, we summarize the potential medical application of wearable EEG systems.

[a] *Department of Biomedical Engineering, The University of Texas at Austin, Austin, TX 78712, USA. E-mail: evanwang@utexas.edu*

[b] *Department of Chemical Engineering, Polytechnique Montréal, Montréal, Québec H3C3J7, Canada*

[c] *Department of Mathematics, The University of Texas at Austin, Austin, TX 78712, USA*

[d] *Department of Aerospace Engineering and Engineering Mechanics, The University of Texas at Austin, Austin, TX 78712, USA*

† These authors contributed equally to this work.

1. Introduction

1.1 Overview of EEG

The electroencephalogram (EEG) is a widely used method for monitoring an individual's brain activity. With electrodes that are highly sensitive to electrical activity, the electrical potential of neuron cells that carries physiological information is recorded. The electrical action potential, the so-called neural spike, is the basic unit of all kinds of brain neural activity, that is important for understanding and monitoring brain functions and neurological diseases.

Ju-Chun Hsieh is currently a PhD student Biomedical Engineering at University of Texas at Austin. He received his MS from National Chiao Tung University in 2019 and BS from National Cheng Kung University in 2017, both in Photonics. His research focuses on the topics of wearable bioelectronics for electrophysiological signals, in particularly broad applications of EEG devices such as brain–computer interfaces (BCIs), epilepsy detection, and sleep monitoring.

Ju-Chun Hsieh

Yang Li currently works at College of Electronic and Optical Engineering and College of Flexible Electronics (Future Technology) in Nanjing University of Posts and Telecommunications. He obtained his BS and MS degree from University of Science and Technology Beijing in 2013 and 2016, respectively. In 2021, he received his PhD degree in chemical engineering from Polytechnique Montreal (affiliated to University of Montreal). His research interests focus on conducting polymers based stretchable and healable electronics, as well as wearable bioelectronics for health monitoring.

Yang Li

To understand the information on brain structure and neural activity, the four main measures are Functional Magnetic Resonance Imaging (fMRI), Magnetoencephalography (MEG), Functional Near-Infrared Spectroscopy (fNIRS), and EEG. The fMRI or fNIRS is a neuroimaging system that measures the changes in blood flow to determine brain function and neural activity. The blood flow is correlated with the electrical neuron activity due to neurovascular coupling. The strength of fMRI and fNIRS are their spatial resolution but lower temporal resolution than EEG due to the direct measurement of neural activity. MEG, on the other hand, maps brain activity by magnetic fields generated from electrical currents occurring in the brain. In comparison to fMRI, MEG could have improved spatial and temporal resolution but both fMRI and MEG are limited by the immobility of the instruments: these equipments are too large to be used as an ambulatory measuring tool. This is hard for user cases in hospitals, not to mention the chance of transferring these techs to home-use health monitoring systems. EEG, on the other hand, has essentially the same signal source as MEG but it is more capable of being a movable measuring instrument through direct measurement of electrical neural activity. Thus, EEG can be a promising method to approach neurological applications, especially considering its high temporal resolution, high versatility, and cost-efficiency. Fig. 1 shows the comparison between these measures of brain activity for their portability, spatial resolution, and temporal resolution.

EEG has been a powerful and popular tool for brain-computer interface (BCI) and event-related potentials (ERPs) research ever since these fields thrived. In recent years, thanks to the blossoming of artificial intelligence and big data in this era and the dramatic evolution of microelectronics as well, EEG applications have expanded from research-oriented tools to more practical use. EEG has become one of the main evaluation tools of brain disease including sleep disorders[1–6] and epileptic
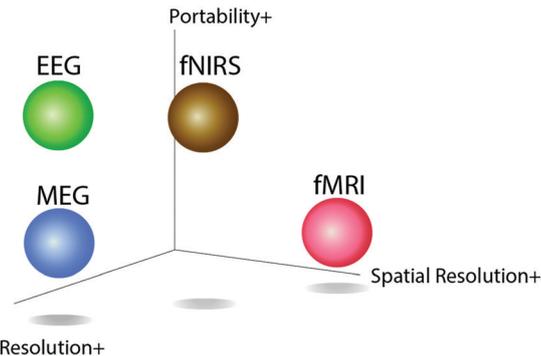

Fig. 1 The comparison between fMRI, MEG, EEG, and fNIRS on their portability, spatial resolution, and temporal resolution. EEG and MEG have the highest temporal resolution, while fMRI has the best spatial resolution. However, to push the wearable brain activity monitoring system forward, portability is critical. EEG and fNIRS both could be developed into portable or wearable devices. Because of the high temporal resolution of EEG, it is now gaining more attention on developing wearable neural activities recording systems.

seizures[7–11] clinically, potential applications in stroke recovery[12–15] and head trauma.[16–19] To date, developers have further extended EEG applications' reach outside of medical use to other fields such as sports training and condition monitoring for athletes,[20–22] robot controls,[23–26] evaluation of driver vigilance.[27,28] Even though these applied technologies have not yet developed to a very mature stage, it shows that more advanced EEG applications are one of the most promising technologies soon.

Conventionally, wired EEG systems are still a mainstay approach to conduct EEG monitoring, both in laboratories or clinics. The current EEG system setup and configuration are elaborated in the following section. Since the wired EEG recording requires numerous wiring connections, the frequent cable disconnections from both ends of electrodes and instrumentation can be extremely frustrating. Furthermore, a wired system must increase the total volume of the system that is directly connected to a subject. Lastly, a conventional EEG system needs a long-winded wet electrode preparation by a trained specialist to ensure the best signal quality of the measurement. As a result, the development of wireless and wearable systems seems to be a reasonable solution to this current situation. A wireless and wearable system also enables experiments and clinical applications that a wired one can never do, for instance, some motion-rich experiments or long-term and continuous disease monitoring while not taking patients out from their daily lives to a hospital.

Bearing all that in mind, developing a wireless and wearable EEG system is a favorable and promising orientation in this field. Prior to this review, numerous independent studies have been done to approach this aim from various angles, which are the driving force of this article. In particular, we focus on the development of wearable EEG hydrogel electrodes that enables advanced wearable EEG recording for medical applications. We start with the conventional setup of EEG systems in medical
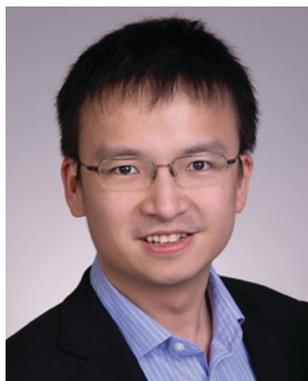
Huiliang Wang

Huiliang (Evan) Wang is an Assistant professor at University of Texas at Austin (UT Austin). Prior to joining UT Austin, he was a postdoc with Karl Deisseroth at Stanford Bioengineering, developing nanomaterial-based technologies for targeted neural modulation. Before then, he had his PhD degree from Stanford Materials Science and Engineering and worked on nanomaterials and polymers for flexible/wearable electronics with Zhenan Bao. He has received several awards and fellowships including the Materials Research Society (MRS) Gold Graduate Student Award, NIH F32 NRSA Postdoctoral Fellowship, NIH K01 Mentored Research Scientist Development Award.

This journal is © The Royal Society of Chemistry 2022

J. Mater. Chem. B, 2022, **10**, 7260–7280 | **7261**

applications, including the meaning of different EEG bands, circuit setup for EEG system, algorithm, and classification. Next, in the "Wearable, hydrogel-based EEG electrode system: a cutting-edge solution", we discuss the important part of data acquisition technology – the electrodes, including over the different types of electrodes including hydrogel electrodes, and figure of merits for designing the electrodes. We will then report the developed wearable EEGs that target the most widely applied brain-related diseases and disorders. For example, BCIs,[29–31] epilepsy diagnosis,[7–11,32,33] sleep disorder diagnosis,[1–6] and mental health evaluation.[34,35]

1.2 Introduction to EEG bands

EEG is the language of the brain, telling the stories of our bodies with electrical signals. For a long time, raw EEG data has been depicted as consisting of several different frequency bands, which are Delta (0.1 to 4 Hz), Theta (4 to 8 Hz), Alpha (8 to 13 Hz), Beta (13 to 30 Hz), and Gamma (greater than 30 Hz). The delta-band is the dominant frequency band during sleep. It helps humans to decrease their awareness toward the outside world, allowing us to enter a deeply relaxed state and enabling us to access the unconscious corner in our brain. The delta-band generally declines during our time of focusing and concentrating states. A disease that is largely related to this band is called Attention Deficit Disorder (ADD). Patients with ADD suffer from focusing because of the increase of delta-band amplitude instead of decrease. Theta-band is more related to the subconsciousness state of the brain and hence often related to the research of memory and emotion[36,37] and sleep monitoring. The alpha-band is the bridge between consciousness and subconsciousness, working as a critical role in the coalescence of brain activity in different frequencies. Alpha-band plays an active role in cognitive processes of brain activity, such as knowledge access and information processing.[38] Beta activity has a long history of relation to Parkinson's disease. The neurodegenerative nature of Parkinson's disease is associated with the neuronal activity in the beta-band. In addition to observing Parkinson's disease by patients' motor impairments, the decreased dopamine release and increased beta-band oscillations are also important indicators. High-frequency Gamma band oscillation in EEG is thought to be a diagnostic biomarker in Alzheimer's disease (AD) and mild cognitive impairment (MCI). The increased gamma-band power has been reported in AD and MCI patients compared to healthy control subjects.[39] To obtain these biomarkers that are hidden in the brainwaves, the EEG measuring system has already been developed for decades and is still being improved and innovative. Next, we introduce the conventional wired measurement system that has been used for a long time in clinics, and the more recent EEG sensing platform, the wireless systems.

1.3 Circuit setup for EEG measurements

An EEG circuit measures the electrical potentials caused by post-synaptic potentials generated by neurons.[40,41] Two electrodes placed on the surface of the skin function together in a manner similar to that of a voltmeter, measuring the strength of the dipole.[40,41] Naturally, the potential encounters several sources of impedance along its journey from the cortex to a processor, with most impedance coming from the outermost layer of the skin, the stratum corneum, in the case of most EEG circuit designs. Contact impedance between EEG electrodes must be greater than 1 kΩ, lest a shortcut is created between them, and below 10 kΩ to ensure a signal can be acquired.[40] The cables connecting the electrodes to the rest of the circuit are often twisted and ultimately blended together to improve electromagnetic compatibility and shielded with a driven guard to reduce current leakage. Of course, a full EEG system could include hundreds of electrodes, so groups of electrodes may feed into a multiplexer, allowing for a selection of inputs, reducing demands on other circuit components.

Ideally, as much of the EEG circuit is housed within a metal container to minimize electronic noise. The use of differential measurements helps to eliminate noise from the signal that would otherwise be caused by electromagnetic interference. A differential amplifier with a common-mode rejection ratio greater than 80 dB is frequently employed to eliminate any signals that appear in both electrodes. Consequently, the inclusion of a differential amplifier, typically an instrumentation amplifier, in an EEG circuit serves to increase the strength of signals of interest while removing noise.[42] An EEG system normally will have a set of amplifiers and band-pass filters in the analog front-end circuit for providing robust and amplified EEG signals to the following steps in the data preprocessing.[43–45] Data acquired *via* the skin electrode(s) will normally first be amplified by analog amplifiers, then processed with a low-pass filter (LPF) and high-pass filter (HPF) to filter out the unwanted signal. In tandem, these filters are used to create a specific range of possible frequencies for data, typically between 0.1 Hz and 100 Hz, but no narrower than 0.5 Hz to 70 Hz. This upper bound is chosen to eliminate the movement artifacts caused by muscles, which normally vary above 100 Hz. The lower bound is chosen to remove artifacts caused by the accumulation of sweat and any minor electrode movements. With the raw data sufficiently attenuated, the data after filtration must now pass through an analog-digital converter (ADC). If the system has a wireless transmission feature, a wireless transmitter module such as Bluetooth is needed for transmitting the collected data to the processors. If the data is in alternating current, an ADC with a 10–12 bit digital resolution may suffice, though a direct current circuit may necessitate a 20-bit digital resolution. The digital signal can be delivered to a processor for analysis such as a laptop or a smartphone in more recent devices.

1.4 Wired and wireless EEG systems

The conventional EEG recording systems in clinical settings are traditionally composed of an EEG headset with metal or Ag/AgCl (silver/silver chloride) electrodes on the corresponding channels. The number of channels on a multichannel EEG recording system can range from 8 to 256 or more (Fig. 2(a)). To collect the EEG signals, the conductive gel will be filled in the space between the scalp and the electrode[46] (Fig. 2(b)). Then, the electrodes are connected to the circuit board with metal wires. These wire connections can be complicated and messy,

7262 | *J. Mater. Chem. B*, 2022, **10**, 7260–7280

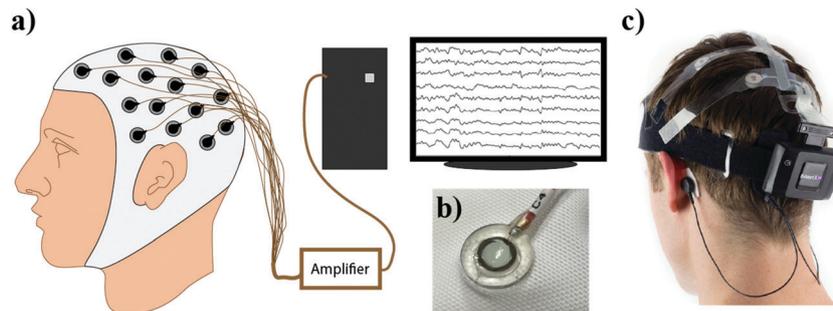This journal is © The Royal Society of Chemistry 2022

Fig. 2 (a) A schematic diagram of a conventional EEG system. (b) A conventional gel–based wet electrode. A wet electrode has a silver/silver chloride electrode and a conductive gel to connect the scalp and the electrode. (c) An example of a wireless system. The image is a B–Alert X24 EEG recording system. Copyright 2010 by Advanced Brain Monitoring, Inc, All Rights Reserved and/or its suppliers. All rights reserved.

and the entire system is far from portable. From wired and cumbersome systems to wireless and portable one, wireless systems allow EEG signals to be acquired with a further shortened preparation time and in a much easier way compared to the traditional system. To date, there are quite a few wireless EEG monitoring systems on the market such as B-Alert X24 and Mindwave, *etc.* As a multi-channel EEG system, the configuration of a wireless system is simpler than the conventional system. Table 1 shows the advantages and disadvantages of wired and wireless systems (Fig. 2(c)). While Mindwave is using dry electrodes for data acquisition, B-Alert X24 is using wet electrodes instead. This is because of the different targeting consumers, while B-Alert is more like a medical/research-grade instrument, Mindwave is targeting daily use or education and entertainment. Owing to the difference in electrodes, the two systems have contrasting setup times. As expected, only 3 minutes to set up for a dry-electrode-use system (Mindwave), and > 20 minutes to set up for a wet-electrode-use system (B-Alert X-24).[47] Even though a wireless system can largely save time for setting up all the wires, we generally still need gels for the electrodes to operate, which is both very time-consuming and does not last for a long time. That brings us to the next topic of this review, cutting-edge technology for the electrodes.

1.5 Data processing and classification

EEG signals are often subjected to a variety of interferences resulting in a heavily noisy bioelectrical signal. Preprocessing steps are necessary to isolate the EEG signal from these noises in order to achieve the most ideal information for post-processing in many applications. However, the removal of all noise in the measurement is impossible. Thus, the best we can do is to remove the major noise components that jeopardize the following steps of signal processing *via* feature extraction and classification.

Typically, the process of EEG-based algorithms on disease prediction and monitoring can be represented in Fig. 3. When the raw EEG data is acquired from a subject, some common noise and artifacts are induced. Fortunately, a well-established foundation of prior studies has already developed a multitude of ways to remove artifacts in EEG data.[48–50] While all these preprocessing methods and toolboxes are well-built and perform greatly in removing artifacts from EEG data, independent component analysis (ICA) has shown to be a common solution to noise/artifact removal. Besides the analysis methods without prior knowledge of a signal such as ICA, the prior-knowledge-based signal decomposition methods are also frequently used in EEG artifacts removal. By having prior knowledge and/or assumptions about the signal of interest and artifacts through physiological understanding in previous studies, the artifacts can be extracted by the design of the signal separation function of an algorithm. For example, wavelet decomposition is regarded as an ideal approach for motion artifact and ocular artifact suppression in EEG.[51–53] With pre-processing being vital in noise removal and signal of interest

Table 1 A comparison between wired systems and wireless wearable systems

	Advantage(s)	Disadvantage(s)
Wired systems	• Connecting to the power system instead of a battery, long-term EEG monitoring can be achieved.	• Complicated wiring.
	• Data security is better than wireless systems.	• Systems can be sometimes bulky and cumbersome.
		• Longer setup time.
		• Not able to be a portable daily-use device but a medical center instrument, which is not conducive to its widespread development.
Wireless systems	• More portable and compact size.	• More external interferences.
	• No wire connection issues.	• The battery capacity and power consumption can largely affect the recording time.
	• Less noise from the wiring.	• Data security can be an issue.
	• Less setup time.	
	• Has a great chance to monitor/record brain activity without being in the medical center (less interruption to daily life).	

This journal is © The Royal Society of Chemistry 2022

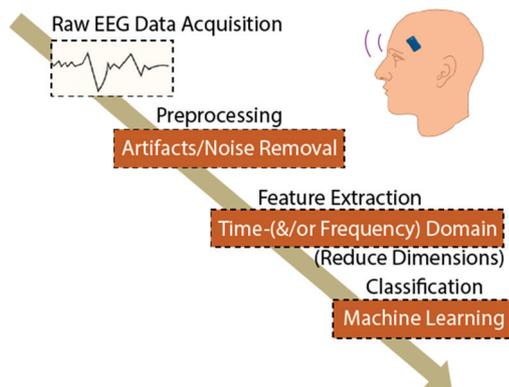*J. Mater. Chem. B*, 2022, **10**, 7260–7280 | **7263**

Fig. 3 The process of EEG-based algorithms on disease prediction and monitoring.

isolation, postprocessing follows subsequently in extracting meaningful data dependent on the aim of the application. Therefore, with feature extraction being a basis in determining feature vector from a regular one in EEG signal analysis, the methods can be mostly, if not all, classified into four categories: (1) non-linear methods,[54] (2) time-domain methods,[55] (3) frequency domain methods[56] and (4) time-frequency domain methods.[56–58]

After feature extraction, diverse EEG classification algorithms will be applied for different medical/clinical applications of EEG systems. All classifiers fall under the category of supervised and unsupervised learning. In supervised learning, such as support vector machines (SVM),[59–62] decision tree (DT),[61,63] random forest (RF),[64,65] and K-nearest neighbor (KNN),[66] the input data is provided along with labelled output data for training the classifier in making accurate predictions. Contrarily, unsupervised learning, such as neural network (NN),[67–70] involves only the input data provided for training the classifier *via* the innate differences in feature vectors extracted from the input.

2. Wearable, hydrogel-based EEG electrode system: a cutting-edge solution

2.1 Categories of EEG electrodes

In order to obtain a high-quality, continuous recording of EEG signals over time, the materials of electrodes are the first priority. Generally, EEG electrodes need to provide good and constant contact with the skin or scalp to lower the impedance. In this section, different types of EEG electrodes are introduced briefly.

2.1.1 Wet electrodes. Wet electrodes are the electrodes accompanied by a conducting gel, which can ensure good electrode/skin contact during EEG measuring.[71] The most well-known wet electrodes are based on Ag/AgCl and are divided into disposable electrodes (Fig. 4(a)) and reusable electrodes (Fig. 4(b)).[72] Another type of wide-used wet electrode is called gold cup electrode (Fig. 4(c)).[73] These electrodes rely

on the use of a conductive gel to help transduce currents from the skin by minimizing the impedance between the skin and the electrode as well as movement of the electrode (Fig. 4(d)).[74] Due to the good conformability, the wet electrode generally can provide low impedance and high-quality EEG signals.

Wet electrodes have previously been adopted to study the overnight sleep EEG signals, while the replacement of the electrodes after each measurement is indispensable, as the dry-out of conducting gel will significantly hamper the recording of high-quality EEG signals.[83] In addition, conducting gel may bring some allergic problem, as skin irritation or rashes sometimes happens to the patients after wearing the wet electrodes for a few hours.[84] As a result, wet electrodes are not suitable for prolonged EEG monitoring for wearable devices due to the high cost of electrodes replacements and issues related to stability and biocompatibility.

Up to now, wet electrodes are still considered as a benchmark of quality to which novel electrodes designs are compared. However, the inconvenience of their application has driven research into alternative electrode designs.[85]

2.1.2 Dry electrodes. Dry electrodes seek to circumvent the need for gel using unique shapes and materials to help transduce currents. This can be accomplished by using small pins to reduce impedance (particularly impedance that might be caused by the hair), at the risk of piercing patient skin, frequently coated in gold to improve conductivity (Fig. 4(e)).[86–88] While these efforts can produce electrodes that are, in some conditions, comparable to Ag/AgCl wet electrodes, these designs are susceptible to half-cell potentials created by sweat that can skew signals, though half-cell potential magnitude has been found to vary with the different metals employed.[89] Other dry electrodes sharing the pin-focused design (albeit sometimes applying different metal coatings) have been found to be more prone to movement artifacts (Fig. 4(f)).[75] Other groups studying similar electrodes have concluded that these designs achieve quality comparable to that of wet electrodes.[90] Many groups noted that these dry electrode designs were far easier to use than wet electrodes, improving their utility for unskilled users.[91–93] However, such electrodes typically make use of long "comb" or "pin" designs to push past hair, which might cause discomfort or even pain during prolonged use.

Other conducting materials, such as gold and microporous titanium,[94–96] conducting polymer poly(3,4-ethylenedioxythiophene) doped with poly(styrene sulfonate) (PEDOT:PSS),[97–99] carbon nanotubes (CNTs),[100] and graphene,[101–103] have also been investigated for their possible use in EEG electrodes. For example, Leleux *et al.* fabricated a flexible EEG electrode *via* depositing PEDOT:PSS on a polyimide substrate and obtain a signal-to-noise ratio (SNR) of 24.4 dB when measuring the somatosensory evoked potentials (Fig. 4(g)).[76] Li *et al.* reported the ultrathin, conformable, and breathable reduced graphene oxide (rGO) electrodes prepared by simultaneous room temperature reduction and patterning process, and achieve an EEG recording with a high fidelity due to the conformal contact with skin (Fig. 4(h)).[77] Yang *et al.* developed an ultrathin (150 nm), ultralightweight (0.24 mg cm^{-2}), self-adhesive,
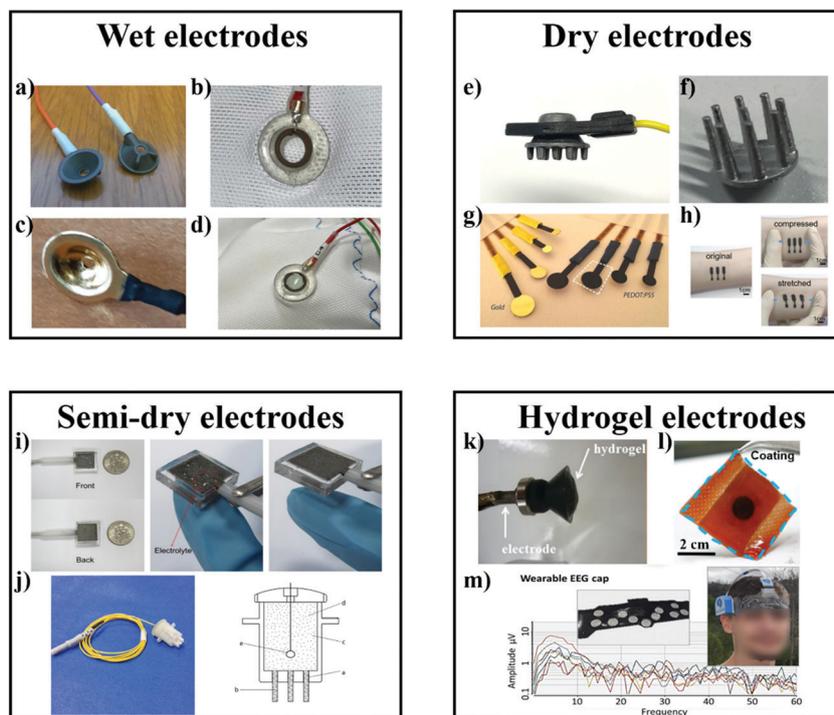
Fig. 4 Different types of EEG electrodes. (a)–(d) Wet electrodes: (a) disposable and (b) reusable silver/silver chloride (Ag/AgCl) passive wet EEG electrodes.[75] (c) Gold cup wet electrode.[73] (d) Close-up of an Ag/AgCl electrode contacting skin *via* a conductive gel. (e)–(h) Dry electrodes: (e) a dry and through-hair EEG sensor. (f) 3D printed EEG electrode coated with silver paint.[75] (g) Photograph of dry PEDOT:PSS electrodes with different diameters.[76] (h) The conformal contact at the skin-rGO electrode interface during compression and stretch.[77] (i) and (j) Semi-dry electrodes: (i) the passive Ti electrode as well as the electrode under pressure and after the pressure removal.[78] (j) Photo of a single semi-dry electrode and schematic diagram of the semi-dry electrode prototype, including flexible electrode tips (a), porous ceramic wicks (b), a built-in reservoir (c), 3.5% saline solution (d), and sintered silver/silver chloride (Ag/AgCl) electrode (e).[79] (k)–(m) Hydrogel electrodes: (k) alginate-based hydrogel electrodes.[80] (l) Photograph of a hydrogel coating on non-woven fabric (commercial bioelectrode with electrolyte hydrogel removed).[81] (m) Headband for signal acquisition with hydrogel electrodes integrated on the textile with printed silver interconnect on the other side of the textile and EEG signals acquired by the headband during sleep.[82]

and transparent Ag nanowire/thermoplastic elastomer electrode, which exhibited a maximum SNR of 51 dB over the wide frequency range of 0–22 000 Hz.[104] Unfortunately, these innovations have yet to consistently match the quality of wet electrodes.

2.1.3 Semi-dry electrodes. Semi-dry electrodes seek to match the accuracy of wet electrodes but minimize the amount of gel required to avoid many of their inconveniences. Efforts to design electrodes that used aqueous electrolyte, rather than gel, to lower impedance produced viable electrodes, though with a life-span insufficient for practical EEG application.[105,106] For instance, Peng *et al.* presented a novel passive electrode based on porous titanium (Ti) and a reservoir with a capacity of 200 μl electrolyte (Fig. 4(i)).[78] The electrolyte in the reservoir will permeate from micro-holes of the porous Ti onto the skin under pressure, providing a continuous wet interface between electrode and skin to maintain low and stable contact impedance. Li *et al.* also reported a novel porous ceramic-based 'semi-dry' electrode whose tips can slowly and continuously release a tiny amount of electrolyte liquid to the scalp, supplying an ionic conducting path for detecting neural signals (Fig. 4(j)).[79] Like research into dry electrodes, semi-dry electrodes have found mixed success, but none have managed to match the standards set by wet electrodes.

2.1.4 Hydrogel or hydrogel-like electrodes. Recently, hydrogel electrodes have shown promise as a possible replacement for the Ag/AgCl wet electrodes often used today. Their high water content and conductive fillers allow for superior conduction.[107–109] Pedrosa *et al.* fabricated a novel alginate-based hydrogel *via* injecting the viscous precursor into the electrode cap cavities and this hydrogel electrode shows no considerable differences between signals acquired with the commercial electrolytic gel during the same *in vivo* EEG acquisition (Fig. 4(k)).[80] The hydrogels possess intrinsic flexibility, which can provide seamless contact with the skin, thus lowering the skin-contact impedance.[110] In addition, the mechanical properties and biocompatibility of hydrogels can be tuned easily, which presents an additional advantage over standard wet electrodes, as hydrogel-based designs are better suited to complement the trend in EEG models towards a more ambulatory design.[109] For example, Wang *et al.* reported a stretchable, conductive, and self-healable polyacrylic acid (PAA) hydrogel electrode, which can capture the EEG data in the quiet and excited state (Fig. 4(l)).[81] Carvalho *et al.* developed various non-drying, skin-adhering, skin-friendly, and transparent electrodes based on glycerol–polyacrylamide hydrogels, and

This journal is © The Royal Society of Chemistry 2022

J. Mater. Chem. B, 2022, **10**, 7260–7280 | **7265**

integrated these electrodes into a series of comfortable e-textiles for wearable monitoring of brain signals through EEG (Fig. 4(m)).[82] In the following section, the figure of merit and recent development of EEG electrodes, with a special emphasis on the hydrogel-like electrodes are reviewed. Electrodes improvements for other bio-potential recordings like electro-cardiogram (ECG) or electromyography (EMG) are reviewed since these could generally be applied as EEG electrodes as well.

2.2 Figure of merit in hydrogel EEG electrodes

In order to understand the advantages and disadvantages of different electrodes, the qualities of interest and the techniques used to measure them must be defined. For the EEG devices, especially for prolonged monitoring, the impedance, adhesion, stability as well as biocompatibility are considered as the most important figures of merit.

2.2.1 Impedance. Impedance refers to the resistance of the electrode to current. A greater impedance causes the electrode to be less sensitive to the signals of interest as well as any noise it might acquire from the patient. The geometric parameters affect the impedance of electrodes, as thicker electrodes or electrodes with a smaller surface possess a higher impedance. However, this is not the only factor that influences an electrode's impedance. For hydrogel electrodes, different electrically conductive fillers, such as conducting polymers, carbon-based materials, or metals are added into the hydrogel matrix

or surface to enhance the conductivity, thus lowering the impedance.[111–113] Majidi et al. incorporated micrometer-sized silver flakes into polyacrylamide-alginate (PAAm-alginate) hydrogel matrix, obtaining a high electrical conductivity (>350 S cm^{-1}) after going through a partial dehydration process, due to the formation of silver flakes percolating networks.[114] Li et al. developed a highly stretchable, self-healing, and degradable multifunctional epidermal sensor assembled from the conductive MXene/amorphous calcium carbonate (ACC)/PAA hydrogels (Fig. 5(a)).[115] The introduction of highly conductive MXene significantly lowers the impedance, leading to a higher SNR (19.96 dB) in EMG testing compared to that of the Ag/AgCl electrodes (0.82 dB) and the commercial electrodes (14.75 dB). Similarly, electrodeposited coatings such as PEDOT:Nafion, PEDOT:PSS, and interfacing with liquid metals like eutectic gallium indium have been applied to the electrode to lower impedance.[116,117] In other cases, coatings of platinum and graphite have been applied to lower the impedance.[118]

Another method to lower the impedance relies on the incorporation of ions, either by soaking hydrogels in the electrolyte solution (two-step solvent exchange) or adding salts into the precursor of hydrogels during synthesis (one-pot synthesis). For instance, increasing the ionic strength by including ionic compounds like salt in that hydrogel electrode lower the impedance.[122] To improve the ionic conductivity, Pan et al. introduced 5 wt% lithium chloride (LiCl) into the
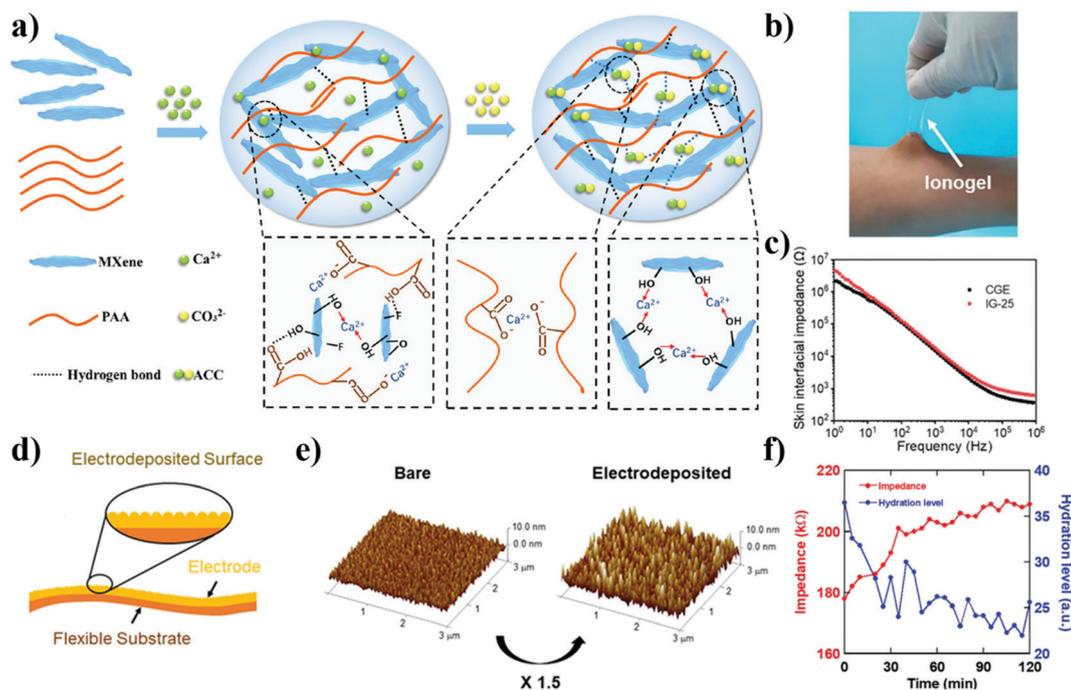

Fig. 5 EEG electrodes with decreased impedance. (a) Schematic illustration of the fabrication of the MXene-PAA-ACC hydrogel.[115] (b) The photos of ionogel electrode adhered to human skin. (c) Skin interfacial impedance of ionogel electrode IG-25 and commercial gel electrode.[119] (d) Schematic of the proposed flexible skin electrode. A gold layer is electrodeposited to maximize the surface area. (e) Atomic force microscopy (AFM) images of bare gold (left) and electrodeposited gold (right) electrodes. The surface area was increased 1.5 times by the electrodeposition process.[120] (f) The relationship between the skin impedance and the hydration level after application of skin lotion.[121]

PAAm-alginate hydrogel.[123] The resulting hydrogel had an intrinsic impedance of 270 Ω (the impedance of the hydrogel without LiCl is $\approx M\Omega$ at 1 Hz), which is similar to commercial electrodes of 210 Ω at 1 Hz. Besides the salts, ionic liquids or polymerized ionic liquids are often adopted to enhance the ionic strength in the electrodes. Yu et al. designed a high-performance and adhesive ionogel by one-step free radical polymerization (Fig. 5(b)).[119] The obtained ionogel electrodes exhibited similar impedance and ECG recording performance as commercial electrodes and provided a continuous and stable ECG monitoring in the aquatic environment due to the strong adhesion to human skin (Fig. 5(c)).

In terms of EEG monitoring, it is worth noting that the outermost layer of the skin, the stratum corneum, is responsible for much of the impedance encountered at the electrode-skin interface in most electrode designs. As a result, skin contact impedance dominates the quality of EEG signals. Of course, skin contact impedance depends on certain factors of skin as well, including the presence of hair follicles and sweat glands, the patient's hydration, temperature, and external force.[124–126]

Electrodes with greater areas of contact with skin typically have a lower impedance.[127,128] This greater surface area of contact manifests in the overall size of the electrode's face as well as its texture-a rougher surface affords a greater surface area. For example, Yun et al. increased the surface area of flexible polyimide substrate by 1.54 times via the electrodeposition of gold nanoparticles (Fig. 5(d) and (e)). Due to the improvement in the surface area, the optimized electrodes demonstrate a higher SNR in ECG and EMG compared to commercial wet Ag/AgCl electrodes.[120] In addition, the surface moisture affects the skin-contact impedance significantly, as high water-ratio hydrogel electrodes can generally hydrate the skin, thus leading to a lower contact impedance. Matsukawa et al. studied the variation of the impedance of gold nanomesh electrodes under different hydration levels, showing that the measured skin impedance was negatively correlated with the hydration level (Fig. 5(f)).[121] Similarly, ions or ionic species released from the electrodes can penetrate the pores of the skin, providing a more conductive skin and better EEG signals. Leleux et al. compared the performance of conformal electrodes made of Au and PEDOT:PSS in a dry state and in conjunction with an ionic liquid gel, discovering that the ionic liquid decreased impedance at the interface with human skin to levels that are similar to those of commercial electrodes (at 1 kHz).[129] In addition, the ionic liquid gel did not dry out and the electrodes continued to show a low impedance over the course of 3 days, while the commercial electrode gave up after only 20 hours. However, high ion concentration inside the recording electrodes may cause skin irritation for patients.

Some preparation methods, such as abrading the skin, using a gel, or wiping the skin with ethanol, may be employed to help reduce the impedance of the skin-electrode interface by partial removal of the stratum corneum. Nevertheless, these methods will generally cause pain for the patients, which is not recommended for long-term monitoring. In the previous reports, additional treatments may make use of penetration enhancers like surfactants, terpenes, and Azones, to reduce the impedance of the skin by altering the hydration of stratum corneum or packing structure of the ordered lipids in the intercellular channels.[130]

2.2.2 Adhesion. The adhesion property of electrodes plays an important role in long-term healthcare monitoring. The electrode for recording EEG signals is directly contacted with human skins or stratum on the head with hair. However, human bodies are easily exposed to various environments (raining, snowing, fog, etc.), and susceptible to human activities like swimming, diving, showering, etc. Besides, mechanical movements such as compression, shear, and torsion are unavoidable in daily life, leading to large deformation of the skin, thus resulting in the loss of EEG signals.[131] High adhesion can provide a seamless contact between the electrodes and skin, thus lowering the impedance and providing stable reliable EEG signals.[132] Therefore, it's crucial for on-skin electrodes to keep adhesive and repetitively usable in daily life and even in extreme environments.

The ways promoting adhesion could be categorized into three directions: (i) functional design of materials, (ii) biomimetic structural design of electrodes, (iii) post-treatment. The adhesion strengthened by these three ways is summarized in Table 2. The functional design aims at creating strong chemical cross-links between electrodes and skin. Among all bonds,

Table 2 Summary of adhesives based on functional design, structural design, and post-treatment

Fabrication method	Materials	Energy toughness (J m^{-2})	Adhesion (kPa)	Ref.
Functional design	DST	>710	120 (Normal)	138
	Ca^{2+} doped PAAm-alginate hydrogel	>1000		140
	PAAm-alginate hydrogel	1250–1500		141
	PAAm + PDMS	866.9		133
Biomimetic structural design	PAA	>750		134
	PDMS	10–50	45–70	142
	PDMS		>120	143
	PDMS		108 (Normal),147 (Shear)	144
	PDMS		25–200 (Normal)	145
	Polyunsaturated aldehyde (PUA)			
Post treatment	PUA		210 (Shear)	146
	Polystyrene	350–1050	>1000 (Shear)	147
	Polypropylene (PP)			148

This journal is © The Royal Society of Chemistry 2022

J. Mater. Chem. B, 2022, **10**, 7260–7280 | **7267**

covalent bonds,[133] hydrogen bonds,[134,135] and electrostatic interactions,[136] are commonly used for the enhancement of on-skin adhesion. A covalent bond has quite high energy, while static covalent bonds are not irreversible, namely, it couldn't reform once the bonds are broken. Dynamic covalent bonds could compensate for such weakness since it is able to reform by pH, light, and heat stimulus. Although a single hydrogen bond is weak, two or more polymer chains can form hydrogen-bonded complexes to strengthen adhesion.[137] Yuk *et al.* proposed a dry double-sided tape (DST) by a combination of gelatin or chitosan and acrylic acid (AA) grafted with *N*-hydroxysuccinimide ester, which removes water from the surface by hydration and forms rapid and robust adhesion with the tissue surface within 5 seconds under pressure at around 1 kPa.[138] Ji *et al.* copolymerized dopamine methacrylamide (DMA), AA, and methoxyethyl acrylate (MEA) monomers to obtain a random copolymer p(DMA-*co*-AA-*co*-MEA) (pDAM) (Fig. 6(a)).[139] Due to the strong adhesion of dopamine-containing motif and ionic conductivity provided by AA, the electrophysiological signals recorded using these
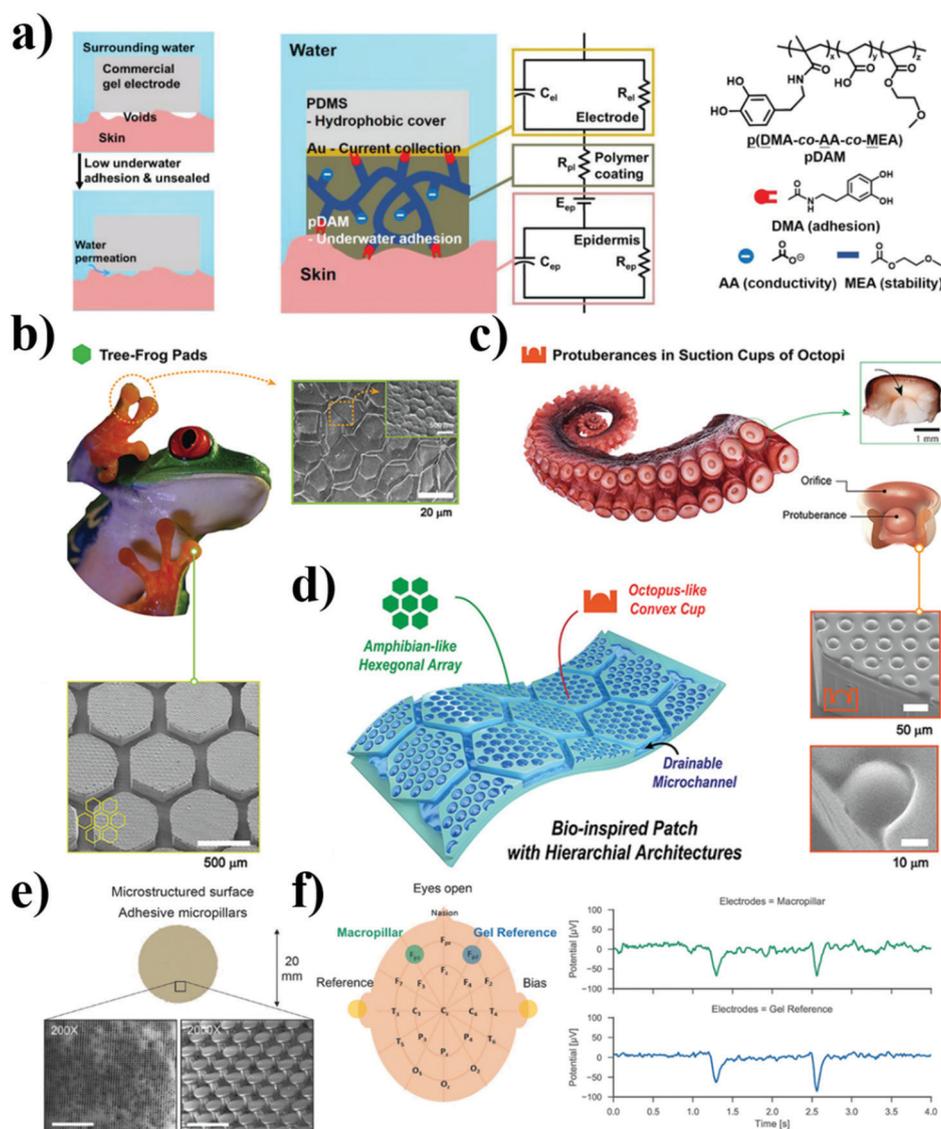

Fig. 6 Possible methods to improve the adhesion of EEG electrodes. (a) Voids exist at the commercial gel electrode–skin interface due to skin surface structure, which allows water in and cause decreased adhesion. Schematic showing the water-resistant pDAM polymer coating bridging the Au/Polydimethylsiloxane (PDMS) electrode and skin, and the corresponding circuit. Chemical structures of the dopamine-containing ionic-conductive random copolymer pDAM.[139] (b) Photograph of pads of a tree frog and scanning electron microscopy (SEM) images of hexagonal structures on its pads and the hierarchical structures (400 μm thickness, PDMS) of frog-inspired hexagonal microchannels (200 μm in width, 300 μm in height, and 600 μm spacing). (c) Photographic images of Octopus vulgaris tentacle and suction cup with protuberance and SEM images of the hierarchical structures with octopus-like convex structures (15 μm in radius and 18 in height) on hexagonal microchannels. (d) Schematic illustration of the amphibian and octopus-like hierarchical architectures.[142] (e) Soft electrode with grasshopper inspired microstructured surface for improved dry adhesion to the skin (thickness = 100 μm). The scale bars are 200 μm (200×) and 20 μm (2000×). (f) The alpha waves disappear when the eyes are kept open. The peaks in the time signal correspond to typical eye blink effects.[149]

7268 | J. Mater. Chem. B, 2022, 10, 7260–7280

This journal is © The Royal Society of Chemistry 2022

water-resistant electrodes were stable and insensitive to the impact of water flow.

Biomimetic structural design is gaining more and more focus in recent years due to its wide application and universality for all materials.[142,150] According to the functions of adhesives in different environments, such a design is divided into wet adhesives inspired by amphibians and marine creatures such as octopus,[142,151] and dry adhesives from insects and lizards like beetles, flies, spiders, geckos, and anole.[144,152,153] For wet adhesives, it has significant adhesive performance as a result of obvious suction force underwater and moisture environment.[145] For example, Kim et al. designed adhesive skin patches with hexagonal micropatterns inspired by the hierarchical microchannel network in the toe pads of tree frogs and convex cup architectures in the suckers of octopi (Fig. 6(b)–(d)).[142] The amphibian- and octopus-like adhesives possess enhanced pulling adhesion and omnidirectional peel resistance against various dynamic wet skins, hence enabling the stable monitoring of vital biosignals. As far as dry adhesives are concerned, the adhesion is enhanced through van der Waals interactions, and the adhesion strength is affected by the tilt angle and the aspect ratio. Stauffer et al. reported super-soft and self-adhesive microstructured electrodes inspired by grasshopper feet, and it could adhere repeatedly to the skin with a force of up to 1 kPa without further attachment even during strong movement or deformation of the skin (Fig. 6(e)).[149] This electrode could obtain excellent alpha activity signals in the EEG recording from the back of the head through dense hair (Fig. 6(f)).

Post-treatment could be classified into two types: chemical modification and plasma treatment. Chemical modification of polymers is aiming to create new chemical groups or moieties that could optimize the polymer matrix to strengthen the adhesion.[154] For instance, alkaline treatment is one of the most common chemical treatments of natural fiber polymer composites. Polymers are dipped into the sodium hydroxide solution for several hours to increase the adhesion by removing impurities like lignin, wax, or oil covering.[155] Plasma treatment is another way to promote surface adhesion between two layers by adjusting the parameters like gas flow, pressure, and treatment time.[148] Dirk et al. used different discharge of gases such as Ar, He, and N_2 to etch, and found that the gas type and plasma conditions have to be adjusted on the polymer type to minimize the aging effects.[156]

2.2.3 Stability. In the context of practical EEG applications, the greatest threat to hydrogel electrode stability is dehydration. Because some amount of water is required for the electrode to properly function, electrodes losing water via evaporation can limit their life span to a few hours, a window of the time insufficient for some EEG applications, such as sleep studies.[157] Not only does water loss reduce the flexibility of hydrogel electrodes, but also increases their impedance.[158]

Encapsulating the hydrogel in an elastomer like polyurethane or latex has been found to reduce dehydration and improve general mechanical stability.[159] Liu et al. sandwich the PAAm-alginate hydrogel in the elastomer PDMS or Ecoflex and

found that the water retention of the hydrogel was around 70% after 6 days still high enough to maintain its function (Fig. 7(a) and (b)).[160] However, the inability to establish a strong bond between the elastomer coating and the hydrogel has prompted exploration into alternatives. As the ions of dissolved salts are known to alter the material properties of gels by interacting with the water molecules, a variety of salts (i.e. $CaCl_2$, NaCl, LiCl, LiBr, et al.) have been explored as additives.[161–163] Bai and colleagues have found that the use of greater salt concentrations and certain salt species such as LiCl, potassium acetate (KAc), and $MgCl_2$ can extend hydrogel electrode lifespan to several days.[164] The best water retention was observed for 12 M LiCl with a cumulative water loss of 11% after 5 days (rel. humidity of environment 20%) (Fig. 7(c)). The higher ionic hydration degree of LiCl enables stronger bond strength between cation/anion-water molecule pairs and more bonded water molecules, resulting in more difficulty of water molecules evaporation and better water retention capacity (Fig. 7(d)).

Water loss was also found to be affected by atmospheric humidity.[167] The fragility and temperature sensitivity of these designs can be mitigated by instead employing an organohydrogel, essentially a hydrogel but formed with a binary solvent consisting of an organic solvent, such as ethylene glycol or glycerol, mixed with water.[168] The inclusion of an organic solvent confers a greater mechanical strength and a greater temperature resistance to the material. Han et al. obtained mussel-inspired glycerol–water hydrogel (GW-hydrogel) with CNTs as conducting nanofillers, via a gelation process in glycerol–water binary-solvent system.[165] The GW-hydrogel exhibited no performance degradation after prolonged storage in normal condition (25 °C) for 30 days (Fig. 7(e)). Similarly, via the exchange of water, ionic liquids can be employed to form ionogels. By radical polymerization of AA in the ionic liquid 1-ethyl-3-methylimidazolium ethylsulfate, Chen et al. synthesized a transparent, stretchable ionogel that might have promise in EEG applications (Fig. 7(f) and (g)).[166] Due to the non-volatility, the ionic liquid and ionogel show much less weight loss and better stability compared to the hydrogels after being in the thermostatic chamber for 12 h (Fig. 7(h)).

All of these solutions have been relatively successful in their endeavor to retain the benefits inherent to hydrogel's flexibility while improving upon its stability. However, further testing is needed to identify if one stands out as clearly superior for the purposes of EEG signal acquisition.[169]

2.2.4 Biocompatibility. To compare the properties of EEG electrodes, biocompatibility refers to the likelihood of an electrode design producing deleterious effects on the patient. For example, the conductive gel required by wet electrodes is an inconvenient irritant that can be difficult to wash off.[170] The metal dry electrodes employ biocompatible materials silver and titanium can be placed on the skin without concern, while the 3D printed components may pose little danger to patients.[171]

However, those designs that rely on breaking the stratum corneum present the risk of damaging the skin or causing pain if designed or applied incorrectly. Pogo probes have been employed to ensure that probes remain in contact without
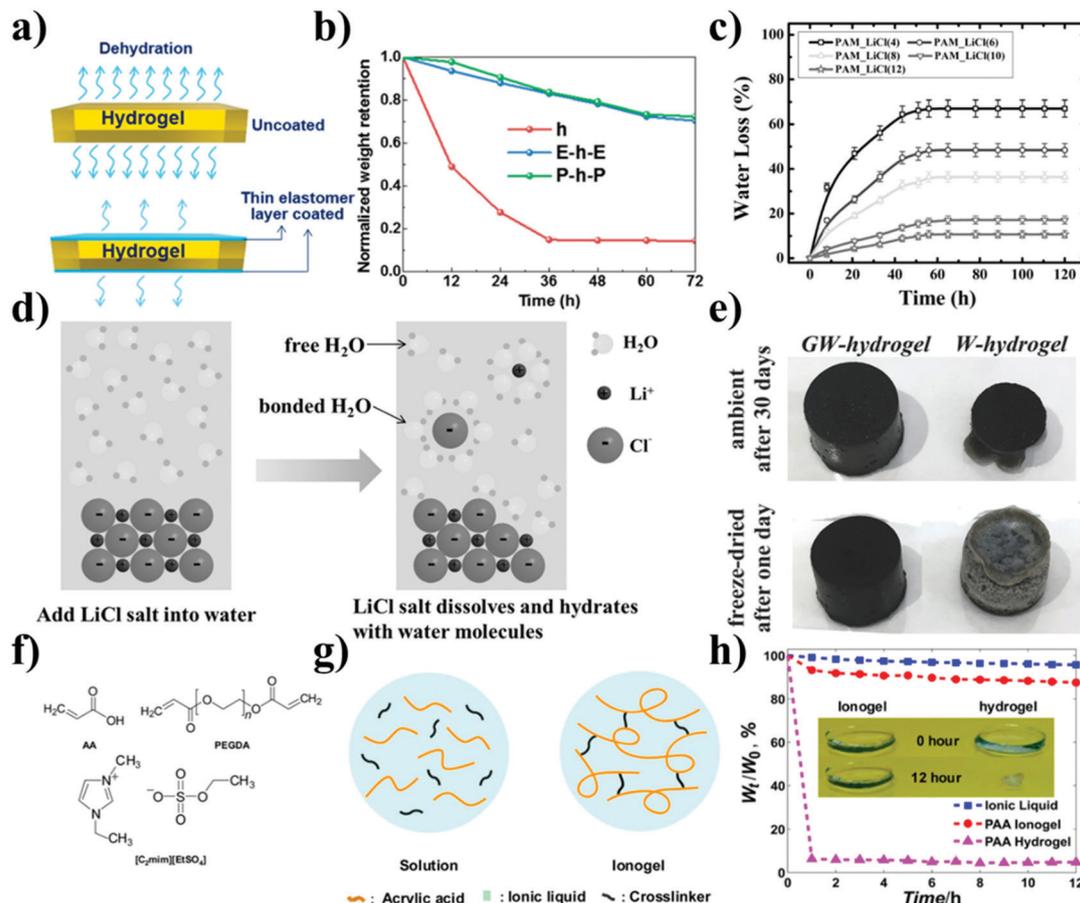
Fig. 7 Possible methods to improve the stability of EEG electrodes. (a) Schematic diagram of the antidehydration of stacked elastomer/hydrogel. (b) Normalized weight retention of the uncoated hydrogel, Ecoflex–hydrogel–Ecoflex (E-h-E), and PDMS–hydrogel–PDMS (P-h-P) kept at a dry environment with a humidity of 26% at 30 °C.[160] (c) Evolution of water loss with time for hydrogel with added LiCl kept in the chamber at 25 °C and relative humidity of 30%. (d) Schematic of the hydration of LiCl in water.[164] (e) Comparison of GW-hydrogels and hydrogels after being placed in air for 30 d or after 1 d of freezing dry.[165] (f) Chemical structure of the hydrogel precursor AA, the crosslinker poly(ethylene glycol) diacrylate (PEGDA), and the ionic liquid 1-ethyl-3-methylimidazolium ethylsulfate. (g) The schematic image of the matrix of the ionogel. (h) Change of weight of the ionic liquid, ionogel and hydrogel in a thermostatic chamber at 100 °C. Inset: Photos of the ionogel, and hydrogel before and after being in the thermostatic chamber for 12 h.[166]

harm, though they can still cause discomfort.[172] Unfortunately, some metal electrode designs prevent water vapor from leaving the skin, causing irritation and inflammation.[121] Gas-permeable nanomeshes have been found to not cause these symptoms by allowing the patient's skin to breathe freely.[173] With this improvement, metal dry electrode designs represent an unequivocal improvement over wet electrodes.

While hydrogel-based designs offer a method to circumvent the need for the conductive gels used in wet electrodes, they offer advantages in other aspects as well. Naturally, hydrogel electrodes offer greater pliability, helping them stay in contact with the skin for longer periods and provide more conduction and improved comfort, as it affords more motion for patients.[174] Furthermore, to improve the biocompatibility, many biocompatible polymers (*i.e.*, polyvinyl alcohol, polyethylene glycol, PAA, chitosan, collagen, *etc.*) have been exploited for either hydrogel-based on-skin applications, causing only mild and even no irritation no reaction at all in either *in vivo* or *in vitro* testing, so it is unlikely that major issues will be encountered in using them.[175–181]

Unfortunately, all of the salt species discussed above have the potential to harm the human body. Although KAc and MgCl$_2$ only present a threat of mild irritation, LiCl, the most promising species can severely burn skin, induce dehydration, and even damage kidneys.[182–184] If salts are to be pursued as a method to improve hydrogel electrode conductivity, special care needs to be taken to either identify less dangerous species or ensure that salts in the hydrogel have no chance of coming into contact with the skin. Of course, the same also applies to any other additives being investigated for use in hydrogel electrodes. While ionogels have not been explored to a similar depth within the context of EEG electrode applications, biocompatible ionogels using compounds like SiO$_2$ are available and might be employed in future research.[185]

2.3 Potential medical applications of hydrogel-based wearable EEG systems

With more and more advancements in hydrogel-based electrodes, the development of wearable EEG systems based on

hydrogel-based electrodes has started to accelerate. Due to the advancement of electrode technology, the quality of the signal is improving over time for applications in wearable EEG systems. We report several potential medical applications that utilized single channel/multichannel EEG systems in the following sections. These applications would benefit from the development of advanced wearable hydrogel-based EEG electrodes. In particular, most of the EEG applications with wet electrodes mentioned need to recalibrate repeatedly in the hospital. The development of hydrogel electrodes will allow wearable EEG systems to be utilized for continuous, long-term EEG monitoring and diagnostics of disease at home.

2.3.1 EEG-based brain-computer interface (BCI). Brain-machine interface (BMI), is a technology that uses the brain's electrical activity for controlling an external device. Given the extreme potential in clinical applications, brain-computer interfaces (BCI) has attracted vast attention recently. Kidnose *et al.* used ear-EEG (Fig. 8(a)) to acquire steady-state visually evoked potential (SSVEP), which has been frequently used for BCI.[29] Norton *et al.* demonstrated a soft and curved electrode system (Fig. 8(b)) for an SSVEP-based BCI text speller system.[30] The electrode system remains mounted throughout daily activities over two weeks, which is a duration that current existing gel-based wet electrodes in clinical settings cannot achieve effectively.

Most recently, Mahmood *et al.* reported a wireless scalp electronic system for motor imagery(MI)-based BCI.[31] With the imperceptible microneedle electrodes (Fig. 8(c)), the study showed an advantageous contact surface area and the reduced electrode impedance density, resulting in great classification accuracy. Combining with the convolutional neural network (CNN), the system realized real-time, continuous motor imagery-based BCI.

To operate a BCI, the user must create various brain activity patterns that the system will recognize through the classification of EEG signals and translate into specific commands. There are also different paradigms of EEG-based BCI such as P300, SSVEP, and MI. The MI paradigm is especially popular in

the stroke rehabilitation field,[186–188] enabling text-to-speech, robotic control, smart wheelchairs, BCI prosthetics, and more,[25,189] as shown in Fig. 8(d).

According to a study from Lotte *et al.*, in the case of performance, adaptive classification techniques should be favored over static techniques, both for classifiers and spatial filters.[190] Adaptive classifiers are those whose parameters are routinely updated online based on the new data to deal with EEG non-stationarity which helps follow changes in EEG features over time and calibration of the BCI system to a specific user. All linear classifiers may be made adaptive, and adaptive SVM has been employed successfully and more frequently in the last decade.[189]

2.3.2 Epilepsy detection. Recording seizures using a wired bulky system can be challenging and hard to be integrated into everyday life. Most of the seizure monitoring sessions need to be done in a medical center. Because of that, many seizures are missed or misreported. People living with epilepsy could benefit by having a miniature, accurate and objective wearable EEG system for counting seizures that can be used outside of the hospital. To date, because of the rapid development of both electrode technologies and algorithms for automatic detection, there are several new miniaturized wearable EEG-based epilepsy monitoring systems come to the public. Frankel *et al.* developed a miniature behind-the-ear epilepsy monitoring system called Epilog. (Fig. 9(a)) To compare this device with the gold standard system, a total of 75 seizures were recorded from 22 of 40 adults that wore Epilog during their visit to the epilepsy monitoring unit. The authors conclude that reviewing single-channel EEG is quick and more accurate ($>70\%$ true positive rate and $>98\%$ positive predictive value) than what has been reported in the literature on self-reporting seizures in seizure diaries, the current standard of care for seizure counting outside of the epilepsy monitoring unit.[191] Swinnen *et al.* used a 2-channel monitoring device, Sensor Dot (SD), to detect typical absence epilepsy in adults and children. (Fig. 9(b)) Blind reading of full SD data resulted in a sensitivity of 81%, a precision of 89%, which is close to the patient self-reporting
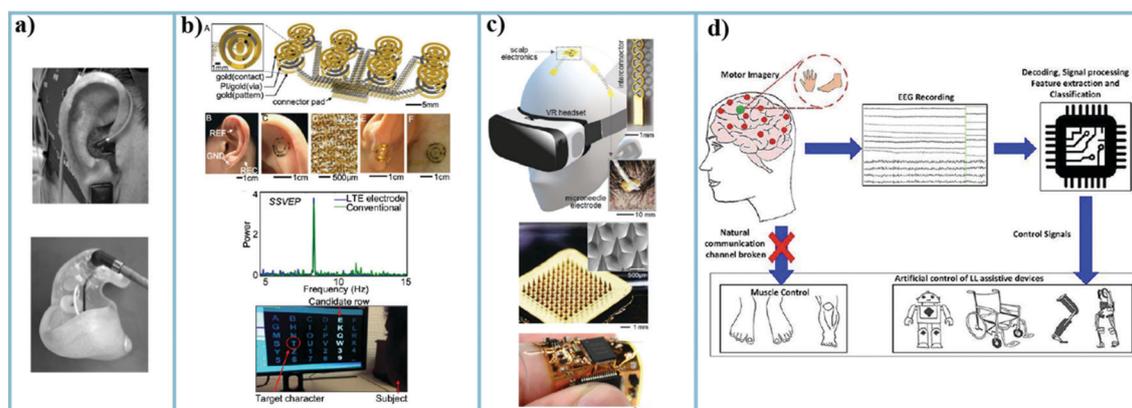

Fig. 8 (a) Images of a subject wearing an earplug Ear-EEG.[29] (b) The schematic diagram of the design of a soft and curved electrode system for an SSVEP-based BCI text speller system.[30] (c) An illustration of a subject wearing the motor-imagery-based scalp EEG electronics with microneedle electrodes and a closeup of stretchable interconnectors.[31] (d) Generic concept diagram of EEG-based BCI controlling assistive devices.[25]

This journal is © The Royal Society of Chemistry 2022

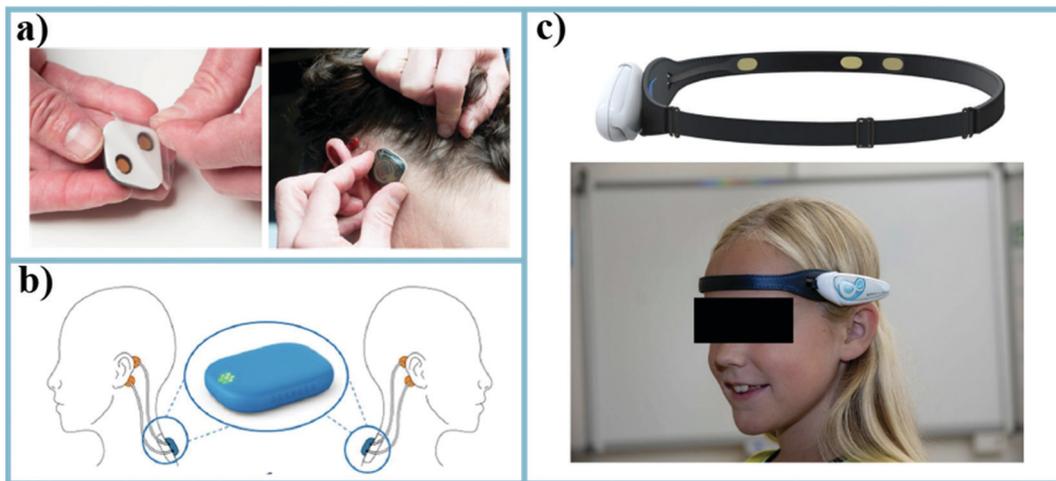*J. Mater. Chem. B*, 2022, **10**, 7260–7280 | **7271**

Fig. 9 Some examples of the newest epilepsy monitoring devices. (a) The Epilog™ miniature wearable EEG sensor uses an adhesive and conductive hydrogel that serves as the interface between Epilog and the scalp when used below the hairline.[191] (b) Four silver/silver chloride standard electrodes (in orange) are placed behind the ears of the patient and connected to Sensor Dot, which is attached to the upper back *via* an adhesive (in blue). An enlarged image of the SD is given in the circle.[192] (c) The BrainLink EEG epileptic seizure monitoring system uses a headband to acquire bipolar signals from the dry electrodes on FP1 and F7.[193]

results, which gave a sensitivity of 80%, precision of 100%.[192] Japaridze *et al.* used the wearable BrainLink EEG to measure the accuracy of fully automated absence seizure detection. (Fig. 9(c)) They recorded 364 absence seizures in 39 patients. The device deficiency was 4.67% and the average sensitivity per patient was 78.83%.[193] The device even correctly documented nonresponsiveness in 30 absence seizures, and responsiveness in six electrographic seizures, which is 100% in the automated behavioral testing in 36 seizures.

Alongside the wearable system, there have been tremendous efforts dedicated to developing generalizable machine learning (ML) algorithms to extract information of epileptic activity in EEG data as well. Recently, many ML methods are applied in the detection of seizures in epilepsy from EEG signals which may be more efficient and consistent than the diagnosis of human physicians. According to the literature, studies related to epilepsy EEG classification tend to use SVM the most, similar to the situation in automatic sleep stage classification (ASSC). Researchers choose other classifiers as well, including ANN, KNN, RF, Naïve-Bayesian (NB), DT, *etc.* In the study by Acharya *et al.* in 2012, the researchers presented a method for automatically detecting normal, pre-ictal, and ictal conditions in recorded EEG signals from the Bonn University dataset.[55] They extracted four entropy-based non-linear features: ApEn, SampEn, S1, and S2 from full time-series EEG data and trained seven classifiers, including FSC (Fuzzy Sugeno Classifier), SVM, KNN, PNN (Probabilistic Neural Network), DT, GMM (Gaussian Mixture Model), and NB. The FSC classifier turned out to outperform the others, which presented the highest accuracy of 98.1%, highest sensitivity of 99.4%, and specificity of 100%. In the case of accuracy, SVM also gained a relatively high performance of 95.9%. We have summarized the classifications that used in epilepsy EEG in Table 3.

2.3.3 Sleep monitoring. Polysomnography (PSG) is the gold standard in evaluating sleep. In the conventional settings of PSGs, sensors for various bioparameters are required, including EEG.[194–196] Due to the issue that PSGs would normally have during the recordings, such as the recording must be in a specialized laboratory and the complicated setup for different biosensors such as ECG, EMG, and Electro-Oculogram (EOG), tremendous efforts have been dedicated to simplifying the sleep monitoring system with portable and wearable EEG systems. The home-based portable and wearable EEGs have gradually emerged in the consumer market, such as Muse S, SleepScope, Neuroon, Dreem headband, SleepShepherd, *etc.* Several validation studies have shown that portable and wearable EEG systems have a good agreement with PSGs.[197,198] Here, we summarize the works in recent years that utilize wearable EEG systems for sleep monitoring and disorder detection, including sleep staging and sleep spindle detection. In 2014, Imtiaz and Rodriguez-Villegas developed an algorithm with a novel feature in sleep EEG to better discern rapid-eye-movement phases from N1 and Wake stages. In their study, they achieved a sensitivity of 83%, specificity of 89%, and selectivity of 61% on a test database consisting of 2221 REM epochs, realizing the automatic detection of REM stages with a single-channel EEG.[194] In addition, Koley and Dey successfully demonstrated the monitoring of sleep from a single channel ear-EEG.[199] while Mikkelsen *et al.* showed that ear-EEG can reliably measure brain activity for sources close to the ear with the same signal-to-noise ratio as scalp.[200] Stochholm, Mikkelsen, and Kidmose applied the same classifier as proposed in a prior work[199] to a single-channel sleep classifier, showing that the performance of the single-channel ear-EEG and a single-channel scalp-EEG have comparable performances.[201] The agreements with the expert manual scoring from each system are 82% for the ear-EEG and 85.7% for the scalp-EEG.

7272 | *J. Mater. Chem. B*, 2022, **10**, 7260–7280

This journal is © The Royal Society of Chemistry 2022

Table 3 Summary of single-channel epilepsy EEG classification

Ref.	Dataset	Classification/accuracy
Lu et al.[8]	Bonn University (five subsets denoted as Z, O, F, N and S)	SVM: 99.00%
Wang et al.[9]	Bonn University (five subsets denoted as Z, O, F, N and S, each group 100 samples)	RF: 96.7%
Siuly and Li[7]	Bonn University (five subsets denoted as Z, O, F, N and S, each group 100 samples)	SVM: 99.96–100% NB: 99.24% KNN: 98.82%
San-Segundo et al.[10]	Bonn University (five subsets denoted as Z, O, F, N and S, each group 100 samples) Note: they also test on another multichannel dataset	NN: 95.6–99.8%
Zhang et al.[11]	Bonn University (five subsets denoted as Z, O, F, N and S, each group 100 samples) Note: the samples were grouped as A, B, C, D, E.	SVM: 80.43%
Wen and Zhang[32]	Bonn University (five subsets denoted as Z, O, F, N and S, each group 100 samples)	KNN: 97.3–98.0% (KNN) DT: 89.7–96.0% (DT) NN: 90.0–97.6% (NN) NB: 82.3–96.7%
	Note: the samples were grouped as A, B, C,D, E.	
Buettner, Frick, and Rieg[33]	Bonn University (five subsets denoted as Z, O, F, N and S, each group 100 samples)	RF: 99.0%

The ear-EEG they used was an earbud-based sensor,[202] which has a similar design as the earplug EEG device that mentioned in Fig. 8(a). About similar time, many of the EEG-based sleep monitoring was investigated based on similar platforms,[200,203–207] as shown in Fig. 10(a). Other body parts like the ear that is not covered by the hair have drawn great attention for the development of EEG-based sleep monitoring systems. A great number of recent sleep studies are focused on acquiring signals from forehead EEGs[208–212] and behind-the-ear EEGs.[213–215] in Fig. 10(b) and (c), respectively.

The system-level progress has benefited from the blossom of the ML algorithms, which boost the developments in the ASSC approach, which would minimize the time requirement of clinicians, increase the diagnostic precision in the classification of sleep stages and improve the treatment for sleep disorders.[216] Here, we give a summary of the most recent and popular classification algorithms in Table 4.

2.3.4 Psychiatry: mental health evaluation. Besides mentioned medical applications, EEG can also be used to detect mild mental issues or major depressive disorder (MDD). EEG signals have been widely used in the studies of antidepressant responses as the relationship between the antidepressant response and the EEG recording for prefrontal cortex activity has drawn tremendous attention.[217–219] However, detecting depression with wearable EEGs has only recently emerged in the field. Li et al. combined linear and nonlinear EEG features to create a 99.1% accuracy classifier for EEG features.[220] They compared the performance of each electrode on the EEG headset to pave the way for the future single-channel wearable EEG system for recording depressions. Cao et al. used a wearable forehead EEG device (Mindo-4S Jellyfish, Eee Holter Technology Co.) to study the responses to ketamine in patients with treatment-resistant depression (TRD).[35] The wearable device is shown in Fig. 11(a). In this study, the authors successfully concluded that the rapid antidepressant effects of mixed doses of ketamine are associated with prefrontal EEG activities, asymmetry, and cordance at baseline and early post-treatment changes. They achieved 81.3% accuracy, 82.1% sensitivity, and 91.9% specificity in classifying responders and non-responders with wearable EEG. Balconi, Fronda, and Crivelli used a wearable EEG system together with ECG to determine the effects of mindfulness exercises on the levels of stress and anxiety of an
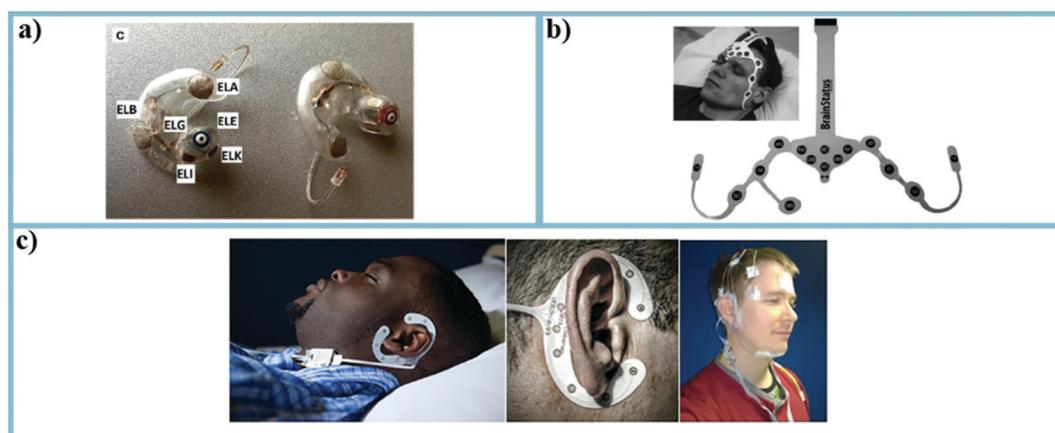

Fig. 10 (a) Based on similar ideas, several works have been developing different types of in-ear EEG-based sleep sensors. This in-ear EEG was first developed by Mikkelsen et al. in 2015.[200] (b) A forehead EEG-based sleep sensor.[212] (c) A set of subjects wearing the recently developed flex-printed around-the-ear electrode array. The figure on the right was the gold standard PSG measurement setup.[214]

This journal is © The Royal Society of Chemistry 2022

J. Mater. Chem. B, 2022, **10**, 7260–7280 | **7273**

Table 4 Summary of single-channel ASSC based on EEG using different classifiers

| Ref.	Dataset	Sleep stages	Channel	Classification/accuracy
Tsinalis et al.[2]	Sleep PSG 20 healthy subjects 20 hour recording per subject	Wake (W), REM (R), non-R stages 1–4 (N1, N2, N3), Movement	Fpz Cz	CNN: 82%
Yücelbaş et al.[6]	17 758 epochs of 28 subjects (21 healthy subjects and 7) obstructive sleep apnea (OSA) patients	Wake (W), non-rapid eye movement (NREM) and rapid eye movement (REM)	Single channel	RF: 78.08% ANN: 70.53% DT: 58.74% NB: 57.31%
da Silveira, Kozakevicius, and Rodrigues[4]	Sleep-EDF database two-night sleep analysis of 10 male and 10 female subjects	All five possible sleep stage arrangements (2–6 state)	Pz-Oz	RF: 90.5–97.3%
Sharma, Pachori, and Upadhyay[3]	Sleep-EDF database eight objects (four healthy, four unhealthy)	All five possible sleep stage arrangements (2–6 state)	Pz-Oz	2 and 6 class state: RF: 98.02% and 89.74% DT: 96.67% and 85.85% KNN: 95.91% and 83.56% NB: 89.01% and 71.8%
Qureshi and Vanichayobon[5]	25 subjects, 21 males and 4 females	W/S1/S2/S3/S4/REM	C4-A1	RF: 97.73% SVM: 93.28%
Zhu, Li, and Wen[1]	Sleep-EDF database 8 subjects	AWA, S1, S2, S3, S4, REM	Pz-Oz	SVM: AWA-REM 96.1% AWA-REM 96.7% S1-REM 75.5% (S1–S2)-SWS 90.6% S1–S2 89.2% S3–S4 77.0%
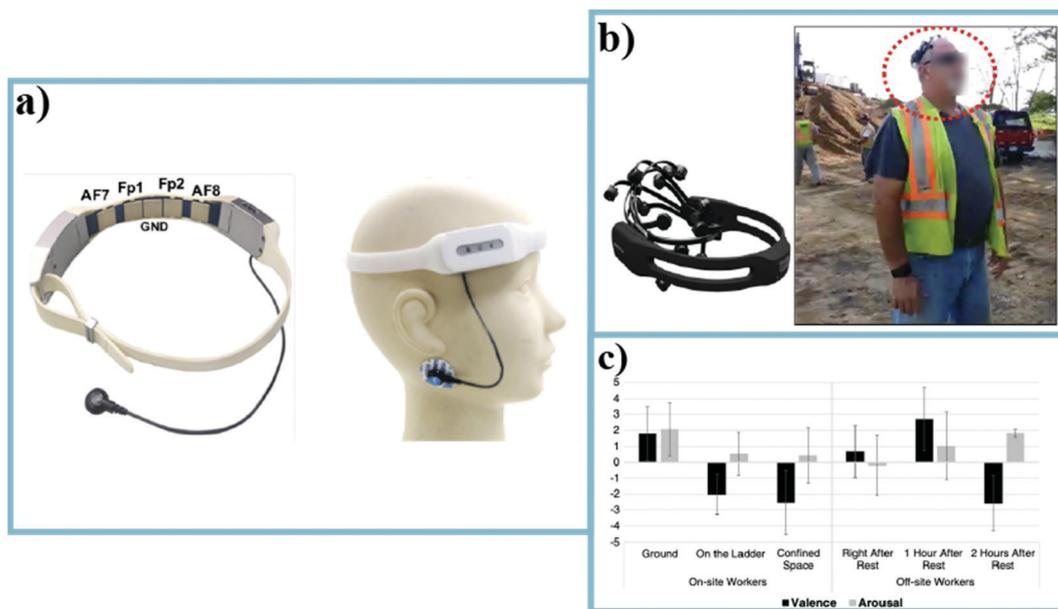
Fig. 11 (a) The wearable forehead EEG device for identifying ketamine responses in treatment-resistant depression.[35] (b) A image of a construction worker wearing a wireless EEG sensor for emotional state measuring.[34] (c) The emotional state monitoring results in different work conditions for on-site and off-site workers after the different amount of working hours: valence and arousal.[34]

individual.[221] The authors concluded that the use of wearable EEG reduced perceived stress and anxiety. Hwang et al. used wearable EEG systems to monitor workers' emotional states during the construction tasks.[34] The study has a bipolar emotional model, consisting of valence and arousal to indicate the emotional state from displeasure to pleasure and from relaxation to excitement, respectively. As Fig. 11(b) and (c) showed, the workers wore the EEG headset under all work conditions,

and the results demonstrated the applicability of a wearable EEG sensor for monitoring workers' mental states.

3. Conclusions and perspectives

Currently, the clinical EEG electrodes are still wet-electrode-based to achieve high-quality recording of EEG signals. However, to maintain prolonged monitoring with wearable EEG

7274 | J. Mater. Chem. B, 2022, **10**, 7260–7280

This journal is © The Royal Society of Chemistry 2022

devices, the impedance, adhesion, stability and biocompatibility are all considered as very important figures of merits. In this review, an emerging type of biopotential electrodes based on hydrogels is discussed. The tunability of hydrogels allows the possibility for the replacement of clinically used Ag/AgCl wet electrodes. With more and more advancements in hydrogel-based electrodes, the hydrogel-based electrodes can be made more versatile according the clinical needs. Here, besides the advancement in the electrodes materials, we also report several different types of EEG electrode systems used for several important medical applications. Majority of these systems are still using standard wet or dry electrodes, but these applications would benefit from the development of advanced wearable hydrogel-based EEG electrodes. Although the challenges of applying hydrogel electrodes to clinical settings still remains, the promising future of the hydrogel-based electrode is undeniable. With the continuous development of the important parameters for hydrogel electrodes technology (including impedance, adhesion, stability and biocompatibility), we believe that hydrogel electrodes based wearable EEG systems will be widely utilized for continuous, long-term EEG monitoring and diagnostics of disease at home.

Conflicts of interest

The authors declare no competing financial interest.

Acknowledgements

References

1 G. Zhu, Y. Li and P. Wen, *IEEE J. Biomed. Health Inform.*, 2014, **18**, 1813–1821.

2 O. Tsinalis, P. M. Matthews, Y. Guo and S. Zafeiriou, *arXiv preprint arXiv:1610.01683*, 2016.

3 R. Sharma, R. B. Pachori and A. Upadhyay, *Neural. Comput. Appl.*, 2017, **28**, 2959–2978.

4 T. L. da Silveira, A. J. Kozakevicius and C. R. Rodrigues, *Med. Biol. Eng. Comput.*, 2017, **55**, 343–352.

5 S. Qureshi and S. Vanichayobon, Evaluate different machine learning techniques for classifying sleep stages on single-channel EEG, In *2017 14th International Joint Conference on Computer Science and Software Engineering (JCSSE)*, IEEE, 2017, pp. 1–6.

6 Ş. Yücelbaş, C. Yücelbaş, G. Tezel, S. Özşen and Ş. Yosunkaya, *Expert Syst. Appl.*, 2018, **102**, 193–206.

7 S. Siuly and Y. Li, *Comput. Methods Programs Biomed.*, 2015, **119**, 29–42.

8 Y. Lu, Y. Ma, C. Chen and Y. Wang, *Technology and Health Care*, 2018, **26**, 337–346.

9 X. Wang, G. Gong, N. Li and S. Qiu, *Front. Hum. Neurosci.*, 2019, **13**, 52.

10 R. San-Segundo, M. Gil-Martín, L. F. D'Haro-Enríquez and J. M. Pardo, *Computers in biology and medicine*, 2019, **109**, 148–158.

11 Y. Zhang, J. Dong, J. Zhu and C. Wu, *IEEE Access*, 2019, **7**, 127600.

12 F. Cincotti, F. Pichiorri, P. Aricò, F. Aloise, F. Leotta, F. de Vico Fallani, J. D. R. Millán, M. Molinari and D. Mattia, EEG-based Brain-Computer Interface to support post-stroke motor rehabilitation of the upper limb, In *2012 Annual International Conference of the IEEE Engineering in Medicine and Biology Society*, IEEE, 2012, pp. 4112–4115.

13 K. K. Ang, K. S. G. Chua, K. S. Phua, C. Wang, Z. Y. Chin, C. W. K. Kuah, W. Low and C. Guan, *Clin. EEG Neurosci.*, 2015, **46**, 310–320.

14 K. K. Ang and C. Guan, *IEEE Trans. Neural Syst. Rehabilitation Eng.*, 2016, **25**, 392–401.

15 R. Foong, K. K. Ang, C. Quek, C. Guan, K. S. Phua, C. W. K. Kuah, V. A. Deshmukh, L. H. L. Yam, D. K. Rajeswaran and N. Tang, *IEEE Trans. Biomed. Eng.*, 2019, **67**, 786–795.

16 J. D. Lewine, S. Plis, A. Ulloa, C. Williams, M. Spitz, J. Foley, K. Paulson, J. Davis, N. Bangera and T. Snyder, *Clin. Neurophysiol.*, 2019, **36**, 298–305.

17 L. L. Popa, H. Dragos, C. Pantelemon, O. V. Rosu and S. Strilciuc, *J Med Life*, 2020, **13**, 8.

18 Y. Kubota, H. Nakamoto, S. Egawa and T. Kawamata, *J. Intensive Care*, 2018, **6**, 1–8.

19 A. Sanz-García, M. Pérez-Romero, J. Pastor, R. G. Sola, L. Vega-Zelaya, F. Monasterio, C. Torrecilla, G. Vega, P. Pulido and G. J. Ortega, *J. Neural Eng.*, 2018, **15**, 066029.

20 K. Thompson, K. Celoch, F. Pizzo, A. I. Fins and J. Tartar, *NeuroSports*, 2020, **1**, 11.

21 D. R. Seshadri, R. T. Li, J. E. Voos, J. R. Rowbottom, C. M. Alfes, C. A. Zorman and C. K. Drummond, *NPJ Digit. Med.*, 2019, **2**, 1–16.

22 E. Butkevičiūtė, L. Bikulčienė, T. Sidekerskienė, T. Blažauskas, R. Maskeliūnas, R. Damaševičius and W. Wei, *IEEE Access*, 2019, **7**, 7206–7217.

23 T. F. Bastos-Filho, *Introduction to Non-Invasive EEG-Based Brain-Computer Interfaces for Assistive Technologies*, CRC Press, 2020.

24 J. H. Cho, J. H. Jeong, K. H. Shim, D. J. Kim and S. W. Lee, Classification of hand motions within EEG signals for non-invasive BCI-based robot hand control, In *2018 IEEE International Conference on Systems, Man, and Cybernetics (SMC)*, IEEE, 2018, pp. 515–518.

25 M. Tariq, P. M. Trivailo and M. Simic, *Front. Hum. Neurosci.*, 2018, 312.

26 A. N. Belkacem and A. Lakas, A Cooperative EEG-based BCI Control System for Robot–Drone Interaction, In *2021 International Wireless Communications and Mobile Computing (IWCMC)*, IEEE, 2021, pp. 297–302.

This journal is © The Royal Society of Chemistry 2022

J. Mater. Chem. B, 2022, **10**, 7260–7280 | **7275**

27 W.-L. Zheng, K. Gao, G. Li, W. Liu, C. Liu, J.-Q. Liu, G. Wang and B.-L. Lu, *IEEE Trans. Intell. Transp. Syst.*, 2019, **21**, 170–184.

28 G. Zhang and A. Etemad, *IEEE Trans. Neural Syst. Rehabilitation Eng.*, 2021, **29**, 1138–1149.

29 P. Kidmose, D. Looney, M. Ungstrup, M. L. Rank and D. P. Mandic, *IEEE Trans. Biomed. Eng.*, 2013, **60**, 2824–2830.

30 J. J. Norton, D. S. Lee, J. W. Lee, W. Lee, O. Kwon, P. Won, S.-Y. Jung, H. Cheng, J.-W. Jeong and A. Akce, *Proc. Natl. Acad. Sci. U. S. A.*, 2015, **112**, 3920–3925.

31 M. Mahmood, S. Kwon, H. Kim, Y. S. Kim, P. Siriaraya, J. Choi, B. Otkhmezuri, K. Kang, K. J. Yu and Y. C. Jang, *Adv. Sci.*, 2021, **8**, 2101129.

32 T. Wen and Z. Zhang, *Medicine*, 2017, **96**(19), DOI: 10.1097/MD.0000000000006879.

33 R. Buettner, J. Frick and T. Rieg, High-performance detection of epilepsy in seizure-free EEG recordings: A novel machine learning approach using very specific epileptic EEG sub-bands, In *ICIS*, 2019.

34 S. Hwang, H. Jebelli, B. Choi, M. Choi and S. Lee, *J. Constr. Eng. Manag.*, 2018, **144**, 04018050.

35 Z. Cao, C.-T. Lin, W. Ding, M.-H. Chen, C.-T. Li and T.-P. Su, *IEEE Trans. Biomed. Eng.*, 2018, **66**, 1668–1679.

36 J. Zheng, R. F. Stevenson, B. A. Mander, L. Mnatsakanyan, F. P. Hsu, S. Vadera, R. T. Knight, M. A. Yassa and J. J. Lin, *Neuron*, 2019, **102**, 887–898.e885.

37 T. Korotkova, A. Ponomarenko, C. K. Monaghan, S. L. Poulter, F. Cacucci, T. Wills, M. E. Hasselmo and C. Lever, *Neurosci. Biobehav. Rev.*, 2018, **85**, 65–80.

38 W. Klimesch, *Trends Cognit. Sci.*, 2012, **16**, 606–617.

39 J. Van Deursen, E. Vuurman, F. Verhey, V. van Kranen-Mastenbroek and W. Riedel, *J. Neural Transm.*, 2008, **115**, 1301–1311.

40 A. B. Usakli, *Comput. Intell. Neurosci.*, 2010, **2010**, DOI: 10.1155/2010/630649.

41 M. A. Lopez-Gordo, D. Sanchez-Morillo and F. P. Valle, *Sensors*, 2014, **14**, 12847–12870.

42 C. S. Wang, *J. Biomed. Biotechnol.*, 2012, **2012**, DOI: 10.1155/2012/274939.

43 J. H. Hong, M. C. Liang, M. Y. Haung, T. H. Tsai, Q. Fang and S. Y. Lee, Analog front-end circuit with low-noise amplifier and high-pass sigma-delta modulator for an EEG or ECoG acquisition system, In *International Symposium on Bioelectronics and Bioinformatics*, IEEE, 2011, pp. 17–20.

44 S. Patki, B. Grundlehner, T. Nakada and J. Penders, Low power wireless EEG headset for BCI applications, In *International Conference on Human-Computer Interaction*, Springer, Berlin, Heidelberg, 2011, pp. 481–490.

45 J. Xu, S. Mitra, A. Matsumoto, S. Patki, C. Van Hoof, K. A. Makinwa and R. F. Yazicioglu, *IEEE, J. Solid State Circ.*, 2014, **49**, 2005–2016.

46 A. J. Casson, *Biomed. Eng. Lett.*, 2019, **9**, 53–71.

47 E. Ratti, S. Waninger, C. Berka, G. Ruffini and A. Verma, *Front. Hum. Neurosci.*, 2017, **11**, 398.

48 A. Delorme and S. Makeig, *J. Neurosci. Methods*, 2004, **134**, 9–21.

49 L. J. Gabard-Durnam, A. S. Mendez Leal, C. L. Wilkinson and A. R. Levin, *Front. Neurosci.*, 2018, **12**, 97.

50 A. Pedroni, A. Bahreini and N. Langer, *NeuroImage*, 2019, **200**, 460–473.

51 G. Inuso, F. La Foresta, N. Mammone and F. C. Morabito, Wavelet-ICA methodology for efficient artifact removal from Electroencephalographic recordings, In *2007 international joint conference on neural networks*, IEEE, 2007, pp. 1524–1529.

52 P. S. Kumar, R. Arumuganathan, K. Sivakumar and C. Vimal, *Int. J. Open Probl. Comput. Math.*, 2008, **1**, 188–200.

53 F. C. Robertson, T. S. Douglas and E. M. Meintjes, *IEEE Trans. Biomed. Eng.*, 2010, **57**, 1377–1387.

54 U. R. Acharya, S. V. Sree, G. Swapna, R. J. Martis and J. S. Suri, *Knowl. Based Syst.*, 2013, **45**, 147–165.

55 U. R. Acharya, F. Molinari, S. V. Sree, S. Chattopadhyay, K.-H. Ng and J. S. Suri, *Biomed. Signal Process*, 2012, **7**, 401–408.

56 A. S. Al-Fahoum and A. A. Al-Fraihat, *Int. Sch. Res. notices*, 2014, **2014**, DOI: 10.1155/2014/730218.

57 K. Rasheed, A. Qayyum, J. Qadir, S. Sivathamboo, P. Kwan, L. Kuhlmann, T. O'Brien and A. Razi, *IEEE Rev. Biomed. Eng.*, 2020, **14**, 139–155.

58 A. Prochazka, J. Kukal and O. Vysata, Wavelet transform use for feature extraction and EEG signal segments classification, In *2008 3rd International symposium on communications, control and signal processing*, IEEE, 2008, pp. 719–722.

59 V. Vapnik, *The nature of statistical learning theory*, Springer science & business media, 1999.

60 S. K. Satapathy and D. Loganathan, *SN Computer Science*, 2021, **2**(3), 1–16.

61 S. Motamedi-Fakhr, M. Moshrefi-Torbati, M. Hill, C. M. Hill and P. R. White, *Biomed. Signal Process*, 2014, **10**, 21–33.

62 M. A. Hearst, S. T. Dumais, E. Osuna, J. Platt and B. Scholkopf, *IEEE Intell. Syst. Appl.*, 1998, **13**, 18–28.

63 J. R. Quinlan, *Mach. Learn.*, 1986, **1**, 81–106.

64 B. Şen, M. Peker, A. Çavuşoğlu and F. V. Çelebi, *J. Med. Syst.*, 2014, **38**, 1–21.

65 Q. Wang, D. Zhao, Y. Wang and X. Hou, *Med. Biol. Eng. Comput.*, 2019, **57**, 1693–1707.

66 D. M. Atallah, M. Badawy and A. El-Sayed, *SN Appl. Sci.*, 2019, **1**, 1–17.

67 M. Hajinoroozi, Z. Mao, T.-P. Jung, C.-T. Lin and Y. Huang, *Signal Process. Image Commun.*, 2016, **47**, 549–555.

68 R. Boostani, F. Karimzadeh and M. Nami, *Comput. Meth. Prog. Bio.*, 2017, **140**, 77–91.

69 J. Han, J. Pei and M. Kamber, *Data mining: concepts and techniques*, Elsevier, 2011.

70 J. Schmidhuber, *Neural networks*, 2015, **61**, 85–117.

71 G. Li, J. Wu, Y. Xia, Y. Wu, Y. Tian, J. Liu, D. Chen and Q. He, *J. Neural Eng.*, 2020, **17**, 026001.

72 A. J. Casson, M. Abdulaal, M. Dulabh, S. Kohli, S. Krachunov and E. Trimble, in *Seamless Healthcare Monitoring: Advancements in Wearable, Attachable, and*

7276 | *J. Mater. Chem. B*, 2022, **10**, 7260–7280

This journal is © The Royal Society of Chemistry 2022

   Invisible Devices, ed. T. Tamura and W. Chen, Springer International Publishing, Cham, 2018, pp. 45–81, DOI: **10.1007/978-3-319-69362-0_2**.

73 G. B. Tseghai, B. Malengier, K. A. Fante and L. V. Langenhove, *Autex Res. J.*, 2021, **21**, 63–70.

74 G. Li, S. Wang and Y. Y. Duan, *Sens. Actuators, B*, 2018, **277**, 250–260.

75 P. Salvo, R. Raedt, E. Carrette, D. Schaubroeck, J. Vanfleteren and L. Cardon, *Sens. Actuators, A*, 2012, **174**, 96–102.

76 P. Leleux, J.-M. Badier, J. Rivnay, C. Bénar, T. Hervé, P. Chauvel and G. G. Malliaras, *Adv. Healthcare Mater.*, 2014, **3**, 490–493.

77 Z. Li, W. Guo, Y. Huang, K. Zhu, H. Yi and H. Wu, *Carbon*, 2020, **164**, 164–170.

78 H.-L. Peng, L. Jing-Quan, H.-C. Tian, Y.-Z. Dong, B. Yang, X. Chen and C.-S. Yang, *Sens. Actuators, B*, 2016, **226**, 349–356.

79 G. Li, D. Zhang, S. Wang and Y. Y. Duan, *Sens. Actuators, B*, 2016, **237**, 167–178.

80 P. Pedrosa, P. Fiedler, L. Schinaia, B. Vasconcelos, A. C. Martins, M. H. Amaral, S. Comani, J. Haueisen and C. Fonseca, *Sens. Actuators, B*, 2017, **247**, 273–283.

81 Q. Wang, X. Pan, C. Lin, X. Ma, S. Cao and Y. Ni, *Chem. Eng. J.*, 2020, **396**, 125341.

82 F. M. Carvalho, P. Lopes, M. Carneiro, A. Serra, J. Coelho, A. T. de Almeida and M. Tavakoli, *ACS Appl. Electron. Mater.*, 2020, **2**, 3390–3401.

83 S. Leach, K. Y. Chung, L. Tüshaus, R. Huber and W. Karlen, *Front. Neurosci.*, 2020, **14**, 586.

84 R. Hajare and S. Kadam, *Global Transitions Proceedings*, 2021, **2**, 467–475.

85 E. H. T. Shad, M. Molinas and T. Ytterdal, *IEEE Sens. J.*, 2020, **20**, 14565–14577.

86 P. Fiedler, R. Mühle, S. Griebel, P. Pedrosa, C. Fonseca, F. Vaz, F. Zanow and J. Haueisen, *IEEE Trans. Neural Syst. Rehabilitation Eng.*, 2018, **26**, 750–757.

87 P. Fiedler, C. Fonseca, E. Supriyanto, F. Zanow and J. Haueisen, *Hum. Brain Mapp.*, 2022, **43**, 1295–1308.

88 R. J. Gentili, K. J. Jaquess, I. M. Shuggi, E. P. Shaw, H. Oh, L.-C. Lo, Y. Y. Tan, C. A. Domingues, J. A. Blanco, J. C. Rietschel, M. W. Miller and B. D. Hatfield, *Psychophysiology*, 2018, **55**, e13059.

89 H. Hinrichs, M. Scholz, A. K. Baum, J. W. Y. Kam, R. T. Knight and H.-J. Heinze, *Sci. Rep.*, 2020, **10**, 5218.

90 G. Di Flumeri, P. Aricò, G. Borghini, N. Sciaraffa, A. Di Florio and F. Babiloni, *Sensors*, 2019, **19**, 1365.

91 G. Pei, J. Wu, D. Chen, G. Guo, S. Liu, M. Hong and T. Yan, *Sensors*, 2018, **18**, 3396.

92 L. Yang, Q. Liu, Z. Zhang, L. Gan, Y. Zhang and J. Wu, *Adv. Mater. Technol.*, 2022, 2100612.

93 A. Harati and A. Jahanshahi, *Sens. Actuators, A*, 2021, **326**, 112727.

94 H. Yuan, Y. Li, J. Yang, H. Li, Q. Yang, C. Guo, S. Zhu and X. Shu, *Micromachines*, 2021, **12**, 1521.

95 W. Liu, W. Zhou, S. Liu, C. Zhang, S. Huang, Y. Li and K. S. Hui, *Sens. Actuators, A*, 2018, **269**, 515–523.

96 G. B. Tseghai, B. Malengier, K. A. Fante and L. V. Langenhove, *IEEE Sens. J.*, 2021, **21**, 22077–22085.

97 D. Khodagholy, J. N. Gelinas, T. Thesen, W. Doyle, O. Devinsky, G. G. Malliaras and G. Buzsáki, *Nat. Neurosci.*, 2015, **18**, 310–315.

98 D. Khodagholy, T. Doublet, P. Quilichini, M. Gurfinkel, P. Leleux, A. Ghestem, E. Ismailova, T. Hervé, S. Sanaur, C. Bernard and G. G. Malliaras, *Nat. Commun.*, 2013, **4**, 1575.

99 G. B. Tseghai, B. Malengier, K. A. Fante, A. B. Nigusse and L. Van Langenhove, *Sensors*, 2020, **20**, 1742.

100 F. La Foresta, F. C. Morabito, S. Marino and S. Dattola, *Electronics*, 2019, **8**, 1031.

101 L. Shao, Y. Guo, W. Liu, T. Sun and D. Wei, *Mater. Res. Express*, 2019, **6**, 085619.

102 L.-W. Ko, C.-H. Su, P.-L. Liao, J.-T. Liang, Y.-H. Tseng and S.-H. Chen, *J. Neural Eng.*, 2021, **18**, 046060.

103 P. Zhai, X. Xuan, H. Li, C. Li, P. Li and M. Li, *Carbon*, 2022, **189**, 71–80.

104 X. Yang, L. Li, S. Wang, Q. Lu, Y. Bai, F. Sun, T. Li, Y. Li, Z. Wang, Y. Zhao, Y. Shi and T. Zhang, *Adv. Electron. Mater.*, 2020, **6**, 2000306.

105 G.-L. Li, J.-T. Wu, Y.-H. Xia, Q.-G. He and H.-G. Jin, *J. Neural Eng.*, 2020, **17**, 051004.

106 H. Hua, W. Tang, X. Xu, D. D. Feng and L. Shu, *Micromachines*, 2019, **10**, 518.

107 N. M. El Ters, A. M. Mathur, S. Jain, Z. A. Vesoulis and J. M. Zempel, *Clin. Neurophysiol.*, 2018, **129**, 1366–1371.

108 G. Shen, K. Gao, N. Zhao, Z. Yi, C. Jiang, B. Yang and J. Liu, *J. Neural Eng.*, 2021, **18**, 066047.

109 Y. Li, X. Zhou, B. Sarkar, N. Gagnon-Lafrenais and F. Cicoira, *Adv. Mater.*, 2022, 2108932.

110 X. Sheng, Z. Qin, H. Xu, X. Shu, G. Gu and X. Zhu, *Sci. China: Technol. Sci.*, 2021, **64**, 273–282.

111 X. Zhou, A. Rajeev, A. Subramanian, Y. Li, N. Rossetti, G. Natale, G. A. Lodygensky and F. Cicoira, *Acta Biomater.*, 2022, **139**, 296–306.

112 B. Lu, H. Yuk, S. Lin, N. Jian, K. Qu, J. Xu and X. Zhao, *Nat. Commun.*, 2019, **10**, 1043.

113 H. Yuk, B. Lu and X. Zhao, *Chem. Soc. Rev.*, 2019, **48**, 1642–1667.

114 Y. Ohm, C. Pan, M. J. Ford, X. Huang, J. Liao and C. Majidi, *Nat. Electron.*, 2021, **4**, 185–192.

115 X. Li, L. He, Y. Li, M. Chao, M. Li, P. Wan and L. Zhang, *ACS Nano*, 2021, **15**, 7765–7773.

116 S. Carli, M. Bianchi, E. Zucchini, M. Di Lauro, M. Prato, M. Murgia, L. Fadiga and F. Biscarini, *Adv. Healthcare Mater.*, 2019, **8**, 1900765.

117 X. Wu, W. Pei, H. Zhang, Y. Chen, X. Guo, H. Chen and S. Wang, *J. Electroanal. Chem.*, 2015, **758**, 26–32.

118 K. Wang, C. L. Frewin, D. Esrafilzadeh, C. Yu, C. Wang, J. J. Pancrazio, M. Romero-Ortega, R. Jalili and G. Wallace, *Adv. Mater.*, 2019, **31**, 1805867.

119 Z. Yu and P. Wu, *Adv. Funct. Mater.*, 2021, **31**, 2107226.

120 I. Yun, J. Jeung, H. Lim, J. Kang, S. Lee, S. Park, S. Seong, S. Park, K. Cho and Y. Chung, *ACS Appl. Electron. Mater.*, 2021, **3**, 1842–1851.

121 R. Matsukawa, A. Miyamoto, T. Yokota and T. Someya, *Adv. Healthcare Mater.*, 2020, **9**, 2001322.

122 T. Shay, O. D. Velev and M. D. Dickey, *Soft Matter*, 2018, **14**, 3296–3303.

123 L. Pan, P. Cai, L. Mei, Y. Cheng, Y. Zeng, M. Wang, T. Wang, Y. Jiang, B. Ji, D. Li and X. Chen, *Adv. Mater.*, 2020, **32**, 2003723.

124 E. S. Kappenman and S. J. Luck, *Psychophysiology*, 2010, **47**, 888–904.

125 B. H. Cornish, B. J. Thomas and L. C. Ward, *Appl. Radiat. Isot.*, 1998, **49**, 475–476.

126 A. Albulbul, *Bioengineering*, 2016, **3**, 20.

127 G. Dijk, H. J. Ruigrok and R. P. O'Connor, *Adv. Mater. Interfaces*, 2020, **7**, 2000675.

128 J. W. Haverkort, *Electrochim. Acta*, 2019, **295**, 846–860.

129 P. Leleux, C. Johnson, X. Strakosas, J. Rivnay, T. Hervé, R. M. Owens and G. G. Malliaras, *Adv. Healthcare Mater.*, 2014, **3**, 1377–1380.

130 P. Karande, A. Jain and S. Mitragotri, *J. Controlled Release*, 2006, **110**, 307–313.

131 Y. Niu, H. Liu, R. He, Z. Li, H. Ren, B. Gao, H. Guo, G. M. Genin and F. Xu, *Mater. Today*, 2020, **41**, 219–242.

132 N. V. de Camp, G. Kalinka and J. Bergeler, *Sci. Rep.*, 2018, **8**, 14041.

133 Q. Liu, G. Nian, C. Yang, S. Qu and Z. Suo, *Nat. Commun.*, 2018, **9**, 846.

134 Y. Wang, K. Jia, C. Xiang, J. Yang, X. Yao and Z. Suo, *ACS Appl. Mater. Interfaces*, 2019, **11**, 40749–40757.

135 P. Song and H. Wang, *Adv. Mater.*, 2020, **32**, 1901244.

136 E. A. Appel, M. W. Tibbitt, J. M. Greer, O. S. Fenton, K. Kreuels, D. G. Anderson and R. Langer, *ACS Macro Lett.*, 2015, **4**, 848–852.

137 J. Yang, R. Bai, B. Chen and Z. Suo, *Adv. Funct. Mater.*, 2020, **30**, 1901693.

138 H. Yuk, C. E. Varela, C. S. Nabzdyk, X. Mao, R. F. Padera, E. T. Roche and X. Zhao, *Nature*, 2019, **575**, 169–174.

139 S. Ji, C. Wan, T. Wang, Q. Li, G. Chen, J. Wang, Z. Liu, H. Yang, X. Liu and X. Chen, *Adv. Mater.*, 2020, **32**, 2001496.

140 J. Li, A. D. Celiz, J. Yang, Q. Yang, I. Wamala, W. Whyte, B. R. Seo, N. V. Vasilyev, J. J. Vlassak, Z. Suo and D. J. Mooney, *Science*, 2017, **357**, 378–381.

141 H. Yuk, T. Zhang, S. Lin, G. A. Parada and X. Zhao, *Nat. Mater.*, 2016, **15**, 190–196.

142 D. W. Kim, S. Baik, H. Min, S. Chun, H. J. Lee, K. H. Kim, J. Y. Lee and C. Pang, *Adv. Funct. Mater.*, 2019, **29**, 1807614.

143 H. Zhang, C. Bian, J. K. Jackson, F. Khademolhosseini, H. M. Burt and M. Chiao, *ACS Appl. Mater. Interfaces*, 2014, **6**, 9126–9133.

144 H. E. Jeong, M. K. Kwak and K. Y. Suh, *Langmuir*, 2010, **26**, 2223–2226.

145 S. Baik, J. Kim, H. J. Lee, T. H. Lee and C. Pang, *Adv. Sci.*, 2018, **5**, 1800100.

146 H. E. Jeong, J.-K. Lee, H. N. Kim, S. H. Moon and K. Y. Suh, *Proc. Natl. Acad. Sci. U. S. A.*, 2009, **106**, 5639–5644.

147 A. Rantell, *Trans. IMF*, 1969, **47**, 197–202.

148 C. Mühlhan, S. Weidner, J. Friedrich and H. Nowack, *Surf. Coat. Technol.*, 1999, **116-119**, 783–787.

149 F. Stauffer, M. Thielen, C. Sauter, S. Chardonnens, S. Bachmann, K. Tybrandt, C. Peters, C. Hierold and J. Vörös, *Adv. Healthcare Mater.*, 2018, **7**, 1700994.

150 S. Kim, J. Wu, A. Carlson, S. H. Jin, A. Kovalsky, P. Glass, Z. Liu, N. Ahmed, S. L. Elgan, W. Chen, P. M. Ferreira, M. Sitti, Y. Huang and J. A. Rogers, *Proc. Natl. Acad. Sci. U. S. A.*, 2010, **107**, 17095–17100.

151 M. K. Choi, O. K. Park, C. Choi, S. Qiao, R. Ghaffari, J. Kim, D. J. Lee, M. Kim, W. Hyun, S. J. Kim, H. J. Hwang, S.-H. Kwon, T. Hyeon, N. Lu and D.-H. Kim, *Adv. Healthcare Mater.*, 2016, **5**, 80–87.

152 Y. Ma, S. Ma, Y. Wu, X. Pei, S. N. Gorb, Z. Wang, W. Liu and F. Zhou, *Adv. Mater.*, 2018, **30**, 1801595.

153 W. R. Hansen and K. Autumn, *Proc. Natl. Acad. Sci. U. S. A.*, 2005, **102**, 385–389.

154 S. Vecchiato, J. Ahrens, A. Pellis, D. Scaini, B. Mueller, E. Herrero Acero and G. M. Guebitz, *ACS Sustainable Chem. Eng.*, 2017, **5**, 6456–6465.

155 R. Agrawal, N. S. Saxena, K. B. Sharma, S. Thomas and M. S. Sreekala, *Mater. Sci. Eng., A*, 2000, **277**, 77–82.

156 D. Hegemann, H. Brunner and C. Oehr, *Nucl. Instrum. Methods Phys. Res., Sect. B*, 2003, **208**, 281–286.

157 A. Markovic, M. Kaess and L. Tarokh, *Sci. Rep.*, 2020, **10**, 15935.

158 Y. Wang, Z. Qu, W. Wang and D. Yu, *Colloids Surf., B*, 2021, **208**, 112088.

159 H. Yuk, T. Zhang, G. A. Parada, X. Liu and X. Zhao, *Nat. Commun.*, 2016, **7**, 12028.

160 T. Liu, M. Liu, S. Dou, J. Sun, Z. Cong, C. Jiang, C. Du, X. Pu, W. Hu and Z. L. Wang, *ACS Nano*, 2018, **12**, 2818–2826.

161 X.-F. Zhang, X. Ma, T. Hou, K. Guo, J. Yin, Z. Wang, L. Shu, M. He and J. Yao, *Angew. Chem., Int. Ed.*, 2019, **58**, 7366–7370.

162 X. P. Morelle, W. R. Illeperuma, K. Tian, R. Bai, Z. Suo and J. J. Vlassak, *Adv. Mater.*, 2018, **30**, 1801541.

163 Z. Wang, J. Cheng, J. Zhou, J. Zhang, H. Huang, J. Yang, Y. Li and B. Wang, *Nano Energy*, 2018, **50**, 106–117.

164 Y. Bai, B. Chen, F. Xiang, J. Zhou, H. Wang and Z. Suo, *Appl. Phys. Lett.*, 2014, **105**, 151903.

165 L. Han, K. Liu, M. Wang, K. Wang, L. Fang, H. Chen, J. Zhou and X. Lu, *Adv. Funct. Mater.*, 2018, **28**, 1704195.

166 B. Chen, J. J. Lu, C. H. Yang, J. H. Yang, J. Zhou, Y. M. Chen and Z. Suo, *ACS Appl. Mater. Interfaces*, 2014, **6**, 7840–7845.

167 X. Zhao, F. Chen, Y. Li, H. Lu, N. Zhang and M. Ma, *Nat. Commun.*, 2018, **9**, 3579.

168 Z. Zhao, K. Zhang, Y. Liu, J. Zhou and M. Liu, *Adv. Mater.*, 2017, **29**, 1701695.

169 D. Zhou, F. Chen, S. Handschuh-Wang, T. Gan, X. Zhou and X. Zhou, *Chem. Phys. Chem.*, 2019, **20**, 2139–2154.

170 J. A. Chiong, H. Tran, Y. Lin, Y. Zheng and Z. Bao, *Adv. Sci.*, 2021, **8**, 2101233.

171 C. F. Guo, Q. Liu, G. Wang, Y. Wang, Z. Shi, Z. Suo, C.-W. Chu and Z. Ren, *Proc. Natl. Acad. Sci. U. S. A.*, 2015, **112**, 12332–12337.

7278 | *J. Mater. Chem. B*, 2022, **10**, 7260–7280

This journal is © The Royal Society of Chemistry 2022

172 S. Lin, J. Liu, W. Li, D. Wang, Y. Huang, C. Jia, Z. Li, M. Murtaza, H. Wang, J. Song, Z. Liu, K. Huang, D. Zu, M. Lei, B. Hong and H. Wu, *Nano Lett.*, 2019, **19**, 6853–6861.

173 A. Miyamoto, S. Lee, N. F. Cooray, S. Lee, M. Mori, N. Matsuhisa, H. Jin, L. Yoda, T. Yokota, A. Itoh, M. Sekino, H. Kawasaki, T. Ebihara, M. Amagai and T. Someya, *Nat. Nanotechnol.*, 2017, **12**, 907–913.

174 J. Wu, Z. Wu, S. Han, B.-R. Yang, X. Gui, K. Tao, C. Liu, J. Miao and L. K. Norford, *ACS Appl. Mater. Interfaces*, 2019, **11**, 2364–2373.

175 N. Alexandre, J. Ribeiro, A. Gärtner, T. Pereira, I. Amorim, J. Fragoso, A. Lopes, J. Fernandes, E. Costa, A. Santos-Silva, M. Rodrigues, J. D. Santos, A. C. Maurício and A. L. Luís, *J. Biomed. Mater. Res., Part A*, 2014, **102**, 4262–4275.

176 X. Jing, H.-Y. Mi, X.-F. Peng and L.-S. Turng, *Carbon*, 2018, **136**, 63–72.

177 P. Moutsatsou, K. Coopman and S. Georgiadou, *Polymers*, 2017, **9**, 687.

178 S. Zhang, Y. Li, G. Tomasello, M. Anthonisen, X. Li, M. Mazzeo, A. Genco, P. Grutter and F. Cicoira, *Adv. Electron. Mater.*, 2019, **5**, 1900191.

179 Y. Li, X. Li, S. Zhang, L. Liu, N. Hamad, S. R. Bobbara, D. Pasini and F. Cicoira, *Adv. Funct. Mater.*, 2020, **30**, 2002853.

180 Y. Li, S. Zhang, X. Li, V. R. N. Unnava and F. Cicoira, *Flexible Printed Electron.*, 2019, **4**, 044004.

181 Y. Li, S. Zhang, N. Hamad, K. Kim, L. Liu, M. Lerond and F. Cicoira, *Macromol. Biosci.*, 2020, **20**, 2000146.

182 K. Feron, R. Lim, C. Sherwood, A. Keynes, A. Brichta and P. C. Dastoor, *Int. J. Mol. Sci.*, 2018, **19**, 2382.

183 D. Gao, K. Parida and P. S. Lee, *Adv. Funct. Mater.*, 2020, **30**, 1907184.

184 M. Torculas, J. Medina, W. Xue and X. Hu, *ACS Biomater. Sci. Eng.*, 2016, **2**, 1211–1223.

185 F. Wang, S. Zhang, Y. Zhang, Q. Lin, Y. Chen, D. Zhu, L. Sun and T. Chen, *Nanomaterials*, 2019, **9**, 343.

186 M. A. Cervera, S. R. Soekadar, J. Ushiba, J. d R. Millán, M. Liu, N. Birbaumer and G. Garipelli, *Annals of clinical and translational neurology*, 2018, **5**, 651–663.

187 A. Biasiucci, R. Leeb, I. Iturrate, S. Perdikis, A. Al-Khodairy, T. Corbet, A. Schnider, T. Schmidlin, H. Zhang and M. Bassolino, *Nat. Commun.*, 2018, **9**, 1–13.

188 L. Tonin and J. d R. Millán, *Annu. Rev. Control Robot. Auton. Syst.*, 2021, **4**, 191–214.

189 R. Janapati, V. Dalal, N. Govardhan and R. S. Gupta, Review on EEG-BCI classification techniques advancements, in *IOP Conference Series: Materials Science and Engineering*, IOP Publishing, 2020, vol. 981, no. 3, p. 032019.

190 F. Lotte, L. Bougrain, A. Cichocki, M. Clerc, M. Congedo, A. Rakotomamonjy and F. Yger, *J. Neural Eng.*, 2018, **15**, 031005.

191 M. A. Frankel, M. J. Lehmkuhle, M. Watson, K. Fetrow, L. Frey, C. Drees and M. C. Spitz, *Clin. Neurophysiol Pract.*, 2021, **6**, 172–178.

192 L. Swinnen, C. Chatzichristos, K. Jansen, L. Lagae, C. Depondt, L. Seynaeve, E. Vancaester, A. Van Dycke, J. Macea and K. Vandecasteele, *Epilepsia*, 2021, **62**, 2741–2752.

193 G. Japaridze, D. Loeckx, T. Buckinx, S. Armand Larsen, R. Proost, K. Jansen, P. MacMullin, N. Paiva, S. Kasradze and A. Rotenberg, *Epilepsia*, 2022, DOI: 10.1111/epi.17200.

194 S. A. Imtiaz and E. Rodriguez-Villegas, *Ann. Biomed. Eng.*, 2014, **42**, 2344–2359.

195 T. Svensson, U.-i Chung, S. Tokuno, M. Nakamura and A. K. Svensson, *J. Psychosom. Res.*, 2019, **126**, 109822.

196 S. Kwon, H. Kim and W.-H. Yeo, *iScience*, 2021, **24**, 102461.

197 M. Yoshida, K. Kashiwagi, H. Kadotani, K. Yamamoto, S. Koike, M. Matsuo, N. Yamada, M. Okawa and Y. Urade, *J. Oral Sleep Med.*, 2015, **1**, 140–147.

198 Z. Liang and M. A. Chapa Martell, *J. Healthc. Inform. Res.*, 2018, **2**, 152–178.

199 B. Koley and D. Dey, *Comput. Biol. Med.*, 2012, **42**, 1186–1195.

200 K. B. Mikkelsen, S. L. Kappel, D. P. Mandic and P. Kidmose, *Front. Neurosci.*, 2015, **9**, 438.

201 A. Stochholm, K. Mikkelsen and P. Kidmose, Automatic sleep stage classification using ear-EEG, In 2016 *38th Annual International Conference of the IEEE Engineering in Medicine and Biology Society (EMBC)*, IEEE, 2016, pp. 4751–4754.

202 D. Looney, V. Goverdovsky, I. Rosenzweig, M. J. Morrell and D. P. Mandic, *Ann. Am. Thorac. Soc.*, 2016, **13**, 2229–2233.

203 K. B. Mikkelsen, D. B. Villadsen, M. Otto and P. Kidmose, *Biomed. Eng. Online*, 2017, **16**, 1–15.

204 T. Nakamura, V. Goverdovsky, M. J. Morrell and D. P. Mandic, *IEEE J. Transl. Eng. Health Med.*, 2017, **5**, 1–8.

205 T. Nakamura, Y. D. Alqurashi, M. J. Morrell and D. P. Mandic, *IEEE Trans. Biomed. Eng.*, 2019, **67**, 203–212.

206 K. B. Mikkelsen, Y. R. Tabar, S. L. Kappel, C. B. Christensen, H. O. Toft, M. C. Hemmsen, M. L. Rank, M. Otto and P. Kidmose, *Sci. Rep.*, 2019, **9**, 1–12.

207 Y. D. Alqurashi, T. Nakamura, V. Goverdovsky, J. Moss, M. I. Polkey, D. P. Mandic and M. J. Morrell, *Nat. Sci. Sleep*, 2018, **10**, 385.

208 C.-T. Lin, C.-H. Chuang, Z. Cao, A. K. Singh, C.-S. Hung, Y.-H. Yu, M. Nascimben, Y.-T. Liu, J.-T. King and T.-P. Su, *IEEE Access*, 2017, **5**, 10612–10621.

209 D. J. Levendowski, L. Ferini-Strambi, C. Gamaldo, M. Cetel, R. Rosenberg and P. R. Westbrook, *J. Clin. Sleep Med.*, 2017, **13**, 791–803.

210 S. Blum, R. Emkes, F. Minow, J. Anlauff, A. Finke and S. Debener, *J. Neural Eng.*, 2020, **17**, 034003.

211 M. R. Carneiro, A. T. de Almeida and M. Tavakoli, *IEEE Sens. J.*, 2020, **20**, 15107–15116.

212 S. Myllymaa, A. Muraja-Murro, S. Westeren-Punnonen, T. Hukkanen, R. Lappalainen, E. Mervaala, J. Töyräs, K. Sipilä and K. Myllymaa, *J. Sleep Res.*, 2016, **25**, 636–645.

213 M. G. Bleichner and S. Debener, *Front. Hum. Neurosci.*, 2017, **11**, 163.

214 A. Sterr, J. K. Ebajemito, K. B. Mikkelsen, M. A. Bonmati-Carrion, N. Santhi, C. Della Monica, L. Grainger, G. Atzori, V. Revell and S. Debener, *Front. Hum. Neurosci.*, 2018, 452.

This journal is © The Royal Society of Chemistry 2022

J. Mater. Chem. B, 2022, **10**, 7260–7280 | **7279**

215 K. B. Mikkelsen, J. K. Ebajemito, M. A. Bonmati-Carrion, N. Santhi, V. L. Revell, G. Atzori, C. Della Monica, S. Debener, D. J. Dijk and A. Sterr, *J. Sleep Res.*, 2019, **28**, e12786.

216 K. A. I. Aboalayon, M. Faezipour, W. S. Almuhammadi and S. Moslehpour, *Entropy*, 2016, **18**, 272.

217 D. V. Iosifescu, S. Greenwald, P. Devlin, D. Mischoulon, J. W. Denninger, J. E. Alpert and M. Fava, *European Neuropsychopharmacology*, 2009, **19**, 772–777.

218 M. Arns, W. H. Drinkenburg, P. B. Fitzgerald and J. L. Kenemans, *Brain Stimul.*, 2012, **5**, 569–576.

219 S. Olbrich and M. Arns, *Int. Rev. Psychiatry*, 2013, **25**, 604–618.

220 X. Li, B. Hu, J. Shen, T. Xu and M. Retcliffe, *J. Med. Syst.*, 2015, **39**, 1–6.

221 M. Balconi, G. Fronda and D. Crivelli, *Stress*, 2019, **22**, 200–209.

7280 | *J. Mater. Chem. B*, 2022, **10**, 7260–7280

This journal is © The Royal Society of Chemistry 2022